

In vivo dosimetry of 3D gynecological brachytherapy using the glass dosimeter: a
phantom study



A Thesis Submitted in Partial Fulfillment of the Requirements
for the Degree of Master of Science in Medical Physics

Department of Radiology

FACULTY OF MEDICINE

Chulalongkorn University

Academic Year 2022

Copyright of Chulalongkorn University

การวัดปริมาณรังสีภายในหุ่นจำลองโดยใช้เครื่องวัดรังสีชนิดแก้วในการรักษาทางนรีเวชด้วยวิธี 3 มิติ



วิทยานิพนธ์นี้เป็นส่วนหนึ่งของการศึกษาตามหลักสูตรปริญญาวิทยาศาสตรมหาบัณฑิต

สาขาวิชาฟิสิกส์การแพทย์ ภาควิชารังสีวิทยา

คณะแพทยศาสตร์ จุฬาลงกรณ์มหาวิทยาลัย

ปีการศึกษา 2565

ลิขสิทธิ์ของจุฬาลงกรณ์มหาวิทยาลัย

Thesis Title *In vivo* dosimetry of 3D gynecological brachytherapy
 using the glass dosimeter: a phantom study

By Miss Itsaraporn Konlak

Field of Study Medical Physics

Thesis Advisor Assistant Professor Taweap Sanghangthum, Ph.D.

Accepted by the FACULTY OF MEDICINE, Chulalongkorn University in Partial
Fulfillment of the Requirement for the Master of Science

----- Dean of the FACULTY OF MEDICINE
(Associate Professor Chanchai Sittipunt, M.D.)

THESIS COMMITTEE

----- Chairman
(Napapat Amornwichee, M.D., Ph.D.)

----- Thesis Advisor
(Assistant Professor Taweap Sanghangthum, Ph.D.)

----- Examiner
(Mintra Keawsamur, Ph.D.)

----- External Examiner
(Professor Franco Milano, Ph.D.)

อิสราภรณ์ คนหลัก : การวัดปริมาณรังสีภายในหุ่นจำลองโดยใช้เครื่องวัดรังสีชนิดแก้วในการรักษา
ทางนรีเวชด้วยวิธี 3 มิติ. (*In vivo dosimetry of 3D gynecological brachytherapy using the
glass dosimeter: a phantom study*) อ.ที่ปรึกษาหลัก : ผศ. ดร.ทวีป แสงแห่งธรรม

การรักษาด้วยรังสีระยะใกล้สามารถให้ปริมาณรังสีที่สูงไปยังบริเวณรอยโรคได้ ในขณะที่เนื้อเยื่อปกติที่อยู่ห่างออกมามีปริมาณรังสีที่ลดลงเนื่องจากอยู่ในบริเวณที่มีการเปลี่ยนแปลงปริมาณรังสีอย่างรวดเร็ว (Steep dose gradient) อย่างไรก็ตามการรักษาดำเนินการตามปริมาณรังสีที่คำนวณโดยระบบการวางแผนการรักษาเท่านั้น โดยไม่มีการตรวจสอบปริมาณรังสีอันเนื่องมาจากลักษณะเฉพาะ ดังนั้นจุดมุ่งหมายของการศึกษานี้คือการออกแบบหุ่นจำลองเพื่อประเมินความแตกต่างของปริมาณรังสีของการรักษาด้วยรังสีระยะใกล้ทางนรีเวชภายใต้เงื่อนไขทางคลินิกระหว่างปริมาณรังสีที่คำนวณได้จากระบบการวางแผนการรักษาและปริมาณรังสีที่วัดได้จากอุปกรณ์วัดรังสีชนิดแก้ว (RPLGD) โดยหุ่นจำลองที่สร้างขึ้นมาประกอบไปด้วยชั้นสำหรับวางอุปกรณ์วัดรังสี RPLGD และตัวยึดสำหรับติดตั้ง applicator ซึ่งสามารถเคลื่อนตำแหน่งแกนของชั้นวางอุปกรณ์วัดรังสี เพื่อใช้สำหรับจุดอ้างอิงลำไส้ตรงที่แตกต่างกันไปตามกายวิภาคของผู้ป่วยแต่ละราย นอกจากนี้ตัวยึด applicator ยังได้รับการออกแบบสำหรับการใช้งานใน applicator ชนิดอื่นๆ ในการรักษาด้วยรังสีระยะใกล้แบบสอดในโพรงร่างกาย (Intracavitary) สำหรับการศึกษาทางคลินิกใช้เพื่อวัดความผันแปรระหว่างปริมาณรังสีที่คำนวณได้และปริมาณรังสีที่วัดได้ ณ จุดอ้างอิงต่างๆ ภายในหุ่นจำลองซึ่งได้แก่จุดอ้างอิง A จุดอ้างอิง B จุดอ้างอิงกระเพาะปัสสาวะและจุดอ้างอิงของลำไส้ตรง เป็นจำนวนทั้งสิ้น 6 เคส โดยความแตกต่างของปริมาณรังสีเฉลี่ยระหว่างปริมาณรังสีที่คำนวณและวัดได้ที่จุดอ้างอิง A คือ 1.99% จุดอ้างอิงกระเพาะปัสสาวะคือ 4.42% และจุดอ้างอิงของลำไส้ตรงคือ 3.53% โดยค่าเฉลี่ยที่กล่าวมาข้างต้นนี้อยู่ภายใน 5% ของค่าอ้างอิงที่ยอมรับได้ สำหรับปริมาณรังสีที่มีค่าต่ำ ณ จุดอ้างอิง B ปริมาณรังสีที่วัดได้จะแตกต่างจากปริมาณรังสีที่คำนวณได้ประมาณ 0.1 Gy สรุปได้ว่าการวัดปริมาณรังสีในหุ่นจำลองโดยใช้อุปกรณ์วัดรังสี RPLGD สำหรับการรักษาด้วยรังสีระยะใกล้ สามารถลดการได้รับปริมาณรังสีเกินขนาดและสามารถประเมินปริมาณรังสีที่ให้แก่ผู้ป่วยโดยใช้อุปกรณ์เสริมสำหรับ applicator ในทางคลินิก

สาขาวิชา ฟิสิกส์การแพทย์
ปีการศึกษา 2565

ลายมือชื่อนิสิต
ลายมือชื่อ อ.ที่ปรึกษาหลัก

6470086430 : MAJOR MEDICAL PHYSICS

KEYWORD:

Itsaraporn Konlak : *In vivo* dosimetry of 3D gynecological brachytherapy using the glass dosimeter: a phantom study. Advisor: Asst. Prof. Taweap Sanghangthum, Ph.D.

Brachytherapy can deliver high doses to the target while sparing healthy tissues due to its steep dose gradient property. However, treatment was only performed according to the dose calculated by a treatment planning system without verification of the dose due to the characteristics. Therefore, the aim of this study was to design the in-house phantom to evaluate the dosimetric differences of gynecological brachytherapy under clinical conditions between calculation by the treatment planning system and measurement by the RPLGDs. An in-house phantom consisting of the glass dosimeter holder and the holder of the applicator was created. This holder was designed to move the axis of the holder to apply the rectum point that differs according to the patient's anatomy. In addition, the holder of the applicator was designed for application in various types of applicators in intracavitary brachytherapy. The clinical study was used to quantify variations between the calculated and measured dose for 6 cases at various points in the phantom, which included point A, point B, bladder point, and rectum points. The mean dose difference between the calculated and measured dose at point A was 1.99%, the bladder point was 4.42%, and the rectum point was 3.53%. All values were within 5% of the acceptable reference value agreement. For the low dose at point B, the measured dose differs from the calculated dose of about 0.1 Gy. We consider that in-vivo dosimetry in the in-house phantom using the RPLGD for brachytherapy can minimize overdoses and, estimate the real delivered dose for the patient's record using an accessory for the applicator in clinical practice.

Field of Study: Medical Physics

Student's Signature

Academic Year: 2022

Advisor's Signature

ACKNOWLEDGEMENTS

I would like to express my sincere gratitude to all the individuals who have helped me throughout the course of my thesis on "In vivo dosimetry of 3D gynecological brachytherapy using the glass dosimeter: a phantom study". Firstly, I would like to convey my heartfelt appreciation to my advisor, Asst. Prof. Taweap Sanghangthum, Ph.D., Division of Radiation Oncology, Department of Radiology, Faculty of Medicine, Chulalongkorn University for his invaluable support, guidance, and constant encouragement throughout the period of my research. His expertise, intellectual guidance, and clear direction have been instrumental in the successful completion of this research. I would also like to extend my gratitude to Mintra Keawsamur, Ph.D., Division of Radiation Oncology, Department of Radiology, King Chulalongkorn Memorial Hospital for her kind suggestions, insightful comments, and shareable her knowledge. I acknowledge with thanks the kind suggestion and good inspiration, which I have received from Mr. Sakda Kingkeaw, Mrs. Chulee Vannavijit, Ms. Nichakan Chatchumnan and all of the staff in the Division of Radiation Oncology, King Chulalongkorn Memorial Hospital for providing their continuous support and for the opportunity to pursue my research in the field of medical physics. Finally, I would like to thank my family and friends for their encouragement, understanding and constant support throughout my research journey. Thank you for your encouragement and support. Without your assistance, this thesis would not have been possible.

Itsaraporn Konlak

TABLE OF CONTENTS

	Page
ABSTRACT (THAI)	iii
ABSTRACT (ENGLISH)	iv
ACKNOWLEDGEMENTS	v
TABLE OF CONTENTS.....	vi
LIST OF FIGURES.....	ix
LIST OF TABLES.....	xi
LIST OF ABBREVIATIONS.....	xii
CHAPTER I INTRODUCTION.....	1
1.1 Background and rationale.....	1
1.2 Objectives	2
CHAPTER II REVIEW OF RELATED LITERATURES.....	3
2.1 Theory	3
2.1.1 Gynecologic cancer.....	3
2.1.2 Brachytherapy	3
2.1.3 Glass dosimeter	6
2.1.4 Three-dimensional printing.....	7
2.1.5 Polylactic acid (PLA)	8
2.2 Review of related literatures	9
CHAPTER III RESEARCH METHODOLOGY.....	15

3.1 Research design	15
3.2 Research design model	15
3.2.1 In-house phantom design	15
3.2.2 Clinical application	16
3.3 Conceptual framework	17
3.4 Research questions	17
3.5 Materials.....	17
3.5.1 The create bot D600 3D printer	17
3.5.2 PLA Filament	18
3.5.3 Shapr3D program	19
3.5.4 The GE CT simulator	20
3.5.5 Elekta Flexitron affterloader	20
3.5.6 The Fletcher applicator	21
3.5.7 Oncentra treatment planning system.....	22
3.5.8 Linear accelerator.....	22
3.5.9 PMMA phantom for brachytherapy	23
3.5.10 Solid water phantom	24
3.5.11 FC-65G and DOSE-I electrometer.....	25
3.5.12 The radio-photoluminescence glass dosimeter (RPLGD).....	25
3.5.13 The automatic reader FGD-1000	26
3.5.14 Carbolite Gero	27
3.6 Methods.....	28
3.6.1 In-house phantom design	28
3.6.2 Clinical application.....	30

3.7 Statistical analysis	36
3.8 Sample size determination	36
3.9 Outcome measurement	37
3.10 Benefits of research	37
3.11 Ethical consideration	37
CHAPTER IV RESULTS.....	38
4.1 In-house phantom design.....	38
4.2 Clinical application	39
4.2.1 Glass dosimeter characteristics	39
4.2.2 Glass dosimeter calibration.....	42
4.2.3 Clinical study.....	42
CHAPTER V DISCUSSION AND CONCLUSION	48
5.1 Discussion	48
5.1.1 In-house phantom design.....	48
5.1.2 Glass dosimeter characteristics	48
5.1.3 Clinical study.....	49
5.2 Conclusion.....	50
REFERENCES.....	51
VITA.....	56

LIST OF FIGURES

	Page
Figure 2.1 Tandem and ovoid (T&O) applicator.....	5
Figure 2.2 Diagram illustrating the dimensions of a glass dosimeter and the principles of dose reading.	7
Figure 2.3 Various densities of 100, 90, 50, 30, and 10% infill cylindrical PLA.....	12
Figure 2.4 (a) Photograph of cuboid specimens with infill of 5%, 20%, 50%, 70%, and 100%. (b) Images of the cubic phantom in the transverse and (c) frontal planes with infill from a CT scan.....	14
Figure 2.5 Mean HU values depend on the 3D printer infill values.....	14
Figure 3.1 Research design model of In-house phantom design.....	15
Figure 3.2 Research design model of clinical study.....	16
Figure 3.3 Conceptual framework.....	17
Figure 3.4 The create bot D600 3D printer.....	18
Figure 3.5 PLA filament.....	19
Figure 3.6 Shapr3D program.....	19
Figure 3.7 The GE CT simulator.....	20
Figure 3.8 Elekta Flexitron affterloader.....	21
Figure 3.9 The Fletcher applicator.....	21
Figure 3.10 Oncentra treatment planning system.....	22
Figure 3.11 Varian TrueBeam linear accelerator.....	23
Figure 3.12 PMMA cylindrical after-loading phantom.....	24
Figure 3.13 Solid water phantom	24

Figure 3.14 FC-65G and DOSE-I electrometer.....	25
Figure 3.15 The radio-photoluminescence glass dosimeter (RPLGD).	26
Figure 3.16 The automatic reader FGD-1000.	27
Figure 3.17 Carbolite Gero.....	27
Figure 3.18 An illustration of the in-house phantom designed in Shapr3D, (a) the glass dosimeter holder, (b) the phantom holder, and (c) the applicator holder.	28
Figure 3.19 The design of all the holders.....	29
Figure 3.20 All the holders of the in-house phantom in the 3D printer process.....	30
Figure 3.21 The in-house phantom setup in the CT scanner.....	30
Figure 3.22 The RPLGD setup position for each experiment.....	31
Figure 3.23 The setup position of the glass dosimeter, and Ir-192 inside the cylindrical PMMA phantom for brachytherapy.....	32
Figure 3.24 The setup position of RPLGD calibration in the cylindrical PMMA phantom.....	33
Figure 3.25 The setup position of the RPLGDs at various points in the in-house phantom, which included point A, point B, bladder, and rectum points.	35
Figure 3. 26 The isodose distribution for the patient plan entered into the in-house phantom.....	35
Figure 4.1 The uniformity of 30 RPLGDs at the dose of 100 cGy. The error bars show the standard deviation from 10 times readout.....	39
Figure 4.2 The reproducibility of the RPLGD. The error bars display the standard deviation from measurements that were taken three times.....	40
Figure 4.3 The time dose linearity response of RPLGD.	41
Figure 4.4 The angular dependence of the RPLGD at different positions in the cylindrical PMMA phantom.	42

LIST OF TABLES

	Page
Table 2.1 Average and standard deviation of five measurements at a single dwell position.....	10
Table 2.2 Measured dose, calculated dose, and compatibility according to locations for the 1004 points.....	11
Table 2.3 CT data for PLA cylinders contrasted against common CT phantoms.....	12
Table 4.1 Measured Hounsfield unit (HU) for various parts of applicators and PLA material.	38
Table 4.2 Difference of energy response to the RPLGD.....	41
Table 4.3 Comparison between dose calculation and measurement at point A.	43
Table 4.4 Comparison between dose calculation and measurement at point B.	44
Table 4.5 Comparison between dose calculation and measurement at bladder point.	45
Table 4.6 Comparison between dose calculation and measurement at rectum point.	46

LIST OF ABBREVIATIONS

Abbreviations	Terms
3D	three dimensional
BT	brachytherapy
cGy	centi -gray
cm	centimeter
CT	computed tomography
Gy	gray
HDR	high dose rate
HR-CTV	high risk -clinical target volume
HU	hounsfield units
IVD	<i>in vivo</i> dosimetry
LDR	low dose rate
MeV	megaelectronvolt
MLC	multileaf collimator
mm	millimeter
MR	magnetic resonance
MU	monitor unit
MV	megavoltage
OAR	organ at risk
ROI	region of interest

RPLGD	radiophotoluminescence glass dosimeter
SSD	source to surface distance
TPS	treatment planning system



CHAPTER I

INTRODUCTION

1.1 Background and rationale

Brachytherapy can deliver high doses to the target while sparing healthy tissues due to its steep dose gradient property, leading to excellent clinical outcomes. However, treatment was only performed according to the dose calculated by a treatment planning system without verification of the dose due to its characteristics, and it is difficult to measure the dose for intracavitary brachytherapy, which has been subject to certain complexities such as CT/MR compatibility with the detector and patient convenience to insert the detector within the body.

To avoid this limitation, phantoms made by using 3D printer materials like PLA, which are robust, long-lasting, are commonly used. This makes it possible to use in vivo dosimetry (IVD) as a direct method of measuring radiation doses, which would verify the dose delivered to the organs at risk and the tumor while the treatment is dispensed. It is important to realize that dose deviations observed between calculated and measured doses can stem from deviations between the planned and delivered dose (clinical effect) or between the delivered and measured dose (measurement uncertainty).

In practice, commercial phantoms cannot be attached simultaneously to the applicator and detector. Thus, in this study, the in-house phantom was designed to evaluate the dosimetric differences of gynecological brachytherapy under clinical conditions between calculation by the treatment planning system and measurement by glass dosimeters.

1.2 Objectives

1.2.1 To design the in-house phantom for *in vivo* dosimetry of 3D gynecological brachytherapy measurement by the glass dosimeter

1.2.2 To evaluate the dosimetric differences of gynecological brachytherapy under clinical conditions between calculation by the treatment planning system and measurement by glass dosimeters.



CHAPTER II

REVIEW OF RELATED LITERATURES

2.1 Theory

2.1.1 Gynecologic cancer

Gynecologic cancer is a type of cancer that affects the female reproductive system, there are several types of gynecologic cancer, including cervical cancer, endometrial cancer, ovarian cancer, vulvar cancer, and vaginal cancer. Treatment of gynecologic cancer usually involves a combination of treatments, including surgery, radiation therapy, chemotherapy, and targeted therapy. Radiation therapy is often used in combination with other types of treatment to increase the chances of recovery. In the case of gynecologic cancer, brachytherapy is often used after external beam radiation therapy (EBRT) to deliver a higher dose of radiation directly to the tumor site. This approach helps to minimize the side effects of radiation therapy while maximizing the effectiveness of treatment.

2.1.2 Brachytherapy

Brachytherapy is the placement of radioactive sources in or just next to a tumor. The word brachytherapy comes from the Greek “brachy” meaning “a close or short distance.” During brachytherapy, the radioactive sources may be left in place permanently or only temporarily, depending upon the tumor. Brachytherapy (BT), or internal radiation therapy, puts a source of radiation in or near cancer. This makes it possible to highly localized radiation dose to the tumor as well as tailor the dose distribution to conform to the shape of the target. BT sources are designed such that the dose fall-off with distance within a tissue is very steep (1). This characteristic of BT sources facilitates the sparing of normal tissues in close proximity to the intended target from receiving a significant amount of radiation dose in contrast to external beam radiation therapy. For this reason, brachytherapy can deliver high doses to the target while sparing healthy tissues due to its steep dose gradient leading to excellent

clinical outcomes(1, 2). There are two types of brachytherapy: low-dose-rate (LDR) and high-dose-rate (HDR). LDR brachytherapy involves permanently or temporarily placing radioactive seeds in the cervical to deliver radiation over an extended period of time, while HDR involves inserting flexible needles into the cervical to deliver a high dose of radiation over a period of a few minutes(3).

2.1.2.1 Brachytherapy technique

Overall, brachytherapy is a highly effective and targeted form of radiation therapy that can be used to treat many different types of cancers. The specific technique used will depend on the location and type of cancer being treated, such as

1. Interstitial brachytherapy involves placing the radioactive sources directly into the tissues surrounding the tumor. This technique is often used to treat prostate cancer, breast cancer, and head and neck cancers.
2. Surface mold brachytherapy involves placing a special mold on the surface of the skin, with radioactive sources embedded within the mold. This technique is used to treat skin cancers or other tumors close to the surface of the skin.
3. Intracavitary brachytherapy is a type of radiation therapy used to treat cancer by placing radioactive sources inside body cavities, such as the vagina, uterus, or esophagus. The radioactive sources are placed in a catheter or applicator, as shown in Fig. 2.1 which is inserted into the body cavity and is typically left in place for a short period of time before being removed. This treatment approach can be used as a standalone treatment or as part of a larger treatment plan, such as in combination with external beam radiation therapy or chemotherapy. The goal of intracavitary brachytherapy is to deliver a high dose of radiation directly to the cancerous cells while minimizing radiation exposure to surrounding healthy tissues.

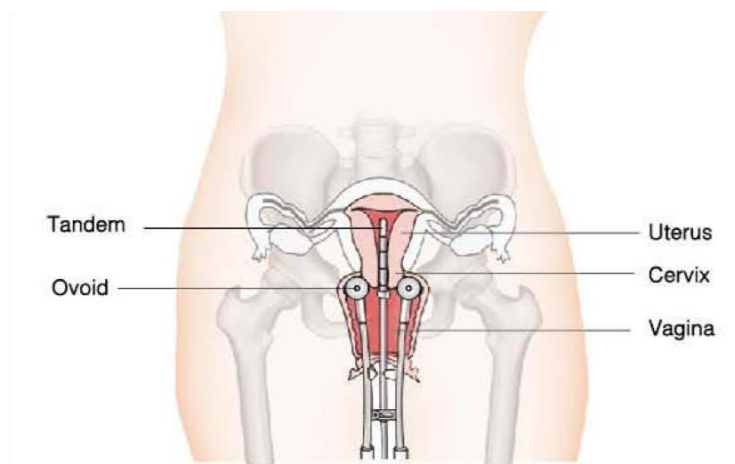


Figure 2.1 Tandem and ovoid (T&O) applicator.

2.1.2.2 Iridium-192 in brachytherapy

Iridium-192 (Ir-192) is the most commonly used source in brachytherapy because of its high specific activity and small size(4). Ir-192 has a half-life of 74 days and is often encased in small pellets, wires, or tubes that are placed directly into the tumor or surrounding tissue. Due to Ir-192 has a high specific activity, or activity per unit mass, which means that a very small source can provide a very high dose rate (HDR), which is essential for HDR applications(5). The radiation is delivered directly to the tumor, allowing for a high dose of radiation to be delivered to cancer while minimizing exposure to surrounding healthy tissue.

2.1.2.3 *In vivo* dosimetry in brachytherapy

In vivo dosimetry means measuring the dose received by the body during a medical procedure, such as radiation therapy or imaging, while the procedure is happening. This is done using specialized devices that can be placed on or inside the body, or by analyzing the patient's biological material. *In vivo* dosimetry provides immediate feedback on the amount of radiation or other energy received, and allows for adjustments to be made during the procedure to ensure optimal dose delivery and minimize the risk of harming healthy tissue.

In vivo dosimetry has been used in brachytherapy for decades and has been referred to International Commission on Radiation Units and Measurements (ICRU) recommendations(2). However, IVD in BT has been subject to certain difficulties and complexities, in particular, due to challenges of the high-gradient BT dose distribution and the large range of dose and dose rate. The initial motivation for performing IVD in BT was mainly to assess doses to organs at risk (OARs) by direct measurements because the precise evaluation of OAR doses was difficult without 3D dose treatment planning.

2.1.3 Glass dosimeter

A radio-photoluminescence glass dosimeter (RPLGD) is a glass compound with a luminescent material. The general composition ratios of the glass for radiation dose measurement are P (31.55%), O (51.16%), Al (6.12%), Na (11.00%), and Ag (0.17%). The density and effective atomic number of the RPLD are 2.61 g/cm^3 and 12.039, respectively(6, 7). When the RPLGD is exposed to ionizing radiation, stable color centers are created(6). Then, the RPLD is excited by an ultraviolet laser beam, the RPL centers return to a stable energy level and emit an orange light. The amount of RPL center (orange light) is proportional to the absorbed dose to the RPLD, as displayed in Figure 2.2. The exposed radiation dose is measured by using the intensity of the light. Because the luminescent centers of the RPLGD are not removed during reading, dose information is eternally preserved, supporting an unlimited number of repeated readouts. If RPLGDs are heated after the dose reading, the accumulated measurement data are reset and reusable.

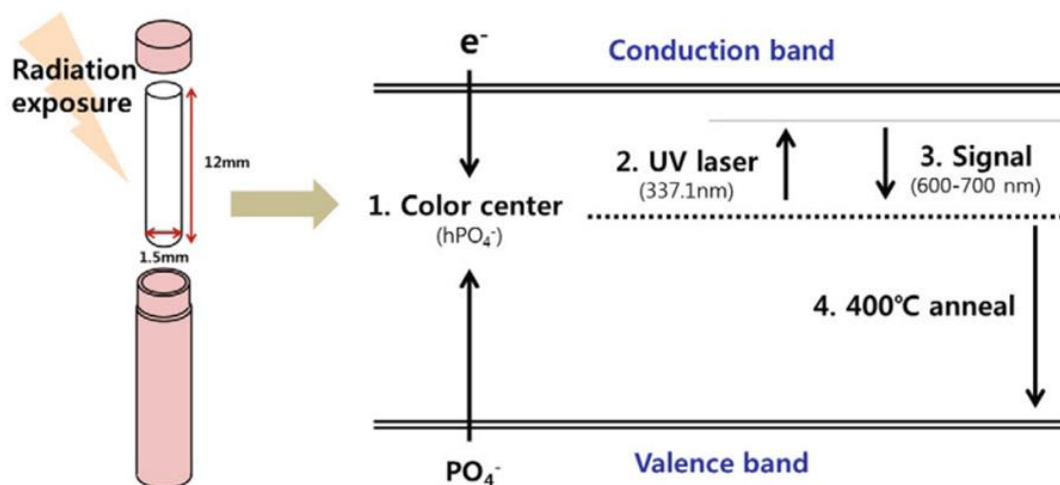


Figure 2.2 Diagram illustrating the dimensions of a glass dosimeter and the principles of dose reading.

2.1.4 Three-dimensional printing

3D printing technology is a process of manufacturing an object in a three-dimensional format using a digital design. The process involves adding layers of material, one layer at a time until the object is formed. The material can include plastic, metal, resin, or even food. The technology allows for great precision and flexibility in creating complex and intricate designs that may be difficult to produce with traditional manufacturing methods.

จุฬาลงกรณ์มหาวิทยาลัย
CHULALONGKORN UNIVERSITY

2.1.4.1 Types of 3D printing

The types of 3D printing can be divided by what they produce or which type of material they use, such as

1. Fused Deposition Modeling (FDM): A type of additive manufacturing that uses a thermoplastic filament, which is melted and extruded in layers to create a 3D object. The print head moves over a build platform to deposit melted material and create the desired shape.

2. Stereolithography (SLA): A type of additive manufacturing that uses a laser to cure a liquid resin one layer at a time. The laser draws the shape of the layer onto the surface of the resin, causing it to harden and bond to the layer below, creating a three-dimensional object.
3. Selective Laser Sintering (SLS): A type of additive manufacturing that uses a laser to selectively melt powdered material, typically nylon, one layer at a time. The laser fuses the particles together, creating a solid layer. The build platform then lowers and a new layer of powder is added, and the process is repeated.
4. Digital Light Processing (DLP): A type of additive manufacturing that uses a light source to cure a liquid resin one layer at a time. A projector shines an image of the layer onto the surface of the resin, causing it to harden and bond to the layer below, creating a three-dimensional object(8).
5. Selective Laser Melting (SLM): A type of additive manufacturing similar to SLS but uses a higher energy laser to completely melt the powdered material, rather than just fusing it together. The melted material solidifies to form the desired shape.
6. Electron beam melting (EBM): A type of additive manufacturing that uses an electron beam to completely melt the powdered material, typically metal. The melted material solidifies to form the desired shape. EBM is commonly used in the aerospace and medical industries for high-strength, bio-compatible parts.

2.1.5 Polylactic acid (PLA)

PLA is a popular 3D printing material used for its ease of use, durability, and environmentally friendly properties. It is a thermoplastic material that is melted and extruded through a 3D printer's nozzle to create the desired shape layer by layer. It has a high melting point, which makes it ideal for printing complex geometries and

intricate designs. Additionally, it has a low warping and shrinkage rate during the printing process, which makes it easy to work with. It is also easily printable with support structures and compatible with many different types of 3D printers. Overall, PLA is an excellent choice for 3D printing, offering ease of use, durability, and environmentally friendly properties.

2.2 Review of related literatures

Moon SY et al.(6) reported the accuracy of dose delivery near the source by inserting glass dosimeters within the applicator. They created an alternative pelvic phantom with the same shape and internal structures as the usual patient and created a tandem for insertion of the glass dosimeters and measured the dose near the source by inserting the glass dosimeters into the tandem. The accuracy of the dwell position and time through the dose near the source were evaluated. The results are shown in Table 2.1. The average and standard deviation of five measurements at a single dwell position. The errors between the values obtained from the five glass dosimeters and the values from the treatment planning system were -6.27, -2.1, -4.18, 6.31, and -0.39%, respectively. The mean error was 3.85%. This value was acceptable considering that the error of the glass dosimeter itself is approximately 3%.

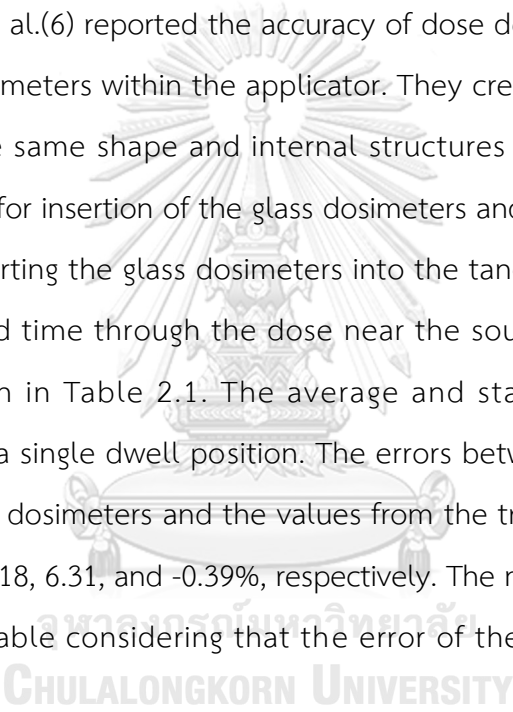


Table 2. 1 Average and standard deviation of five measurements at a single dwell position.

GD #	Glass dosimeter		TPS (cGy)	Error (%)
	Average (cGy)	Standard Deviation (%)		
A	3465.79	3.44	3697.47	-6.27
B	11861.41	8.24	12116.1	-2.1
C	2690.02	2.4	2807.26	-4.18
D	4206.92	5.14	3957.24	6.31
E	2583.11	2.86	2593.19	-0.39

Nose T et al.(9) performed the largest in vivo dosimetry study for interstitial brachytherapy yet to be undertaken using a new radiophotoluminescence glass dosimeter (RPLGD) in patients with pelvic malignancy and studied the limits of contemporary planning software based on the results. Doses for a total of 1004 points in sixty-six patients with pelvic malignancy were treated with high-dose-rate interstitial brachytherapy, including prostate (n = 26), gynecological (n = 35), and miscellaneous (n = 5) were measured by RPLGDs and calculated with planning software in the following locations: rectum (n = 549), urethra (n = 415), vagina (n = 25), and perineum (n = 15). The compatibility (measured dose/calculated dose) was analyzed according to the dosimeter location. The results are shown in Table 2.2. The compatibility for all dosimeters was 0.98 ± 0.23 , stratified by location: rectum, 0.99 ± 0.20 ; urethra, 0.96 ± 0.26 ; vagina, 0.91 ± 0.08 ; and perineum, 1.25 ± 0.32 . Deviations between measured and calculated doses for the rectum and urethra were greater than 20%, which is attributable to the independent movements of these organs and the applicators. Missing corrections for inhomogeneity are responsible for the 9% negative shift near the vaginal cylinder (specific gravity = 1.24), whereas

neglect of transit dose contributes to the 25% positive shift in the perineal dose. Dose deviation of >20% for nontarget organs should be taken into account in the planning process.

Further development of planning software and a real-time dosimetry system is necessary to use the current findings and achieve adaptive dose delivery.

Table 2.2 Measured dose, calculated dose, and compatibility according to locations for the 1004 points.

Region	Measured dose	Calculated dose	Compatibility ratio*
Anterior wall of the rectum (<i>n</i> = 549)	17.6 Gy (3.7–64.6 Gy)	18.3 Gy (3.2–75.7 Gy)	0.99 ± 0.20
Urethra (<i>n</i> = 415)	20.5 Gy (3.7 Gy-88.7 Gy)	21.7 Gy (2.6 Gy-78.8 Gy)	0.96 ± 0.26
Male urethra (<i>n</i> = 181)	28.3 Gy (4.1 Gy-88.7 Gy)	36.7 Gy (3.4 Gy-78.8 Gy)	0.90 ± 0.30
Female urethra (<i>n</i> = 234)	17.5 Gy (3.7 Gy-71.7 Gy)	18.2 Gy (2.6–73.0 Gy)	1.01 ± 0.20
Vaginal wall (<i>n</i> = 25)	38.8 Gy (9.5 Gy-82.4 Gy)	43.0 Gy (9.0–94.7 Gy)	0.91 ± 0.08
Perineal skin (<i>n</i> = 15)	6.9 Gy (3.7 Gy-59.6 Gy)	6.3 Gy (2.4–61.6 Gy)	1.25 ± 0.32
Total (<i>n</i> = 1004)	18.6 Gy (3.7 Gy-88.7Gy)	19.9 Gy (2.4–94.7 Gy)	0.98 ± 0.23

Van der Walt M et al.(10) evaluated the suitability of PLA as a 3D thermoplastic to be used clinically in a radiotherapy department. They created customized cylindrical phantoms using infill densities of 100, 90, 50, 30, and 10% in 3D printer, as displayed in Figure 2.3. From the measured data in Table 2.3, it was found that the various PLA cylinders exhibit relative electron densities and linear attenuation values consistent with the range of known commercially available tissue phantoms. They found similar results for their PLA cylinders when converting from RED to physical mass density. The data from Table 2.3 shows that when deviating from 100% infill, we can expect correction factors from 1.026–1.077 depending on infill density.

Comparative analysis has shown that varying degrees of infill % PLA the thermoplastic can simulate materials in the relative electron density range 0.01–1.10. It was determined that PLA samples could be accurately modeled in the Monaco

TPS, and also found that PLA samples could retain their physical properties even after exposure to a substantial number of monitor units (MUs) wover several weeks.

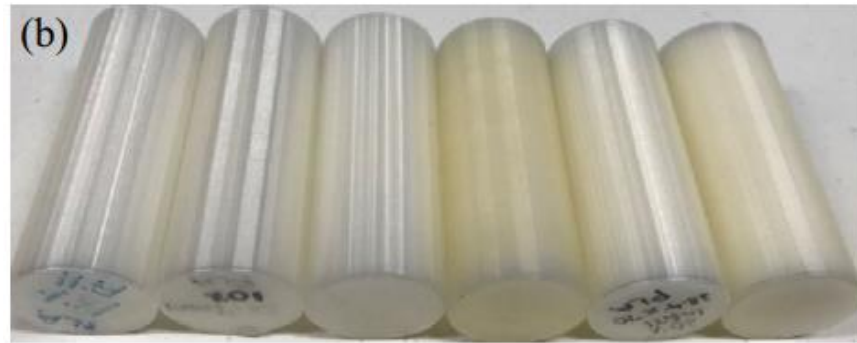


Figure 2.3 Various densities of 100, 90, 50, 30, and 10% infill cylindrical PLA.

Table 2.3 CT data for PLA cylinders contrasted against common CT phantoms.

Phantom	ρ_{calc} (g/cm ³)	ρ_{meas} (g/cm ³)	RED	REDEff	HU	μ (rel)
Cylinder—100% PLA	1.170 ± 0.007	1.173	1.085 ± 0.007	1.058 ± 0.01	138 ± 12	1.128 ± 0.007
Cylinder—90% PLA	0.983 ± 0.017	1.009	0.963 ± 0.017	0.956 ± 0.01	-39 ± 17	0.965 ± 0.017
Cylinder—50% PLA	0.545 ± 0.017	0.564	0.527 ± 0.017	0.555 ± 0.01	-482 ± 17	0.531 ± 0.017
Cylinder—30% PLA	0.318 ± 0.017	0.344	0.317 ± 0.017	0.382 ± 0.01	-693 ± 17	0.320 ± 0.017
Cylinder—10% PLA	0.086 ± 0.090	0.111	0.113 ± 0.090	-	-898 ± 90	0.124 ± 0.090
Dancewicz et al. 90% PLA	-	1.04 ± 0.03	1.01 ± 0.03	-	8 ± 4	-
Dancewicz et al. 50% PLA	-	0.550 ± 0.05	0.540 ± 0.05	-	-	-
CT-ED Brain Model #481	-	1.049	1.009 ± 0.009	-	8 ± 10	-
CT-ED Liver	-	1.039	1.055 ± 0.005	-	89 ± 8	1.089 ± 0.005
CT-ED Cortical Bone	-	1.819	1.712 ± 0.012	-	1207 ± 20	2.207 ± 0.012
CT-ED Adipose	-	0.920	0.922 ± 0.01	-	-100 ± 20	0.900 ± 0.01
CT-ED Lung 300	-	0.300	0.312 ± 0.026	-	-690 ± 80	0.310 ± 0.026
CT-ED Lung 450	-	0.450	0.427 ± 0.026	-	-560 ± 80	0.440 ± 0.026
CT-ED Breast Model	-	0.980	0.957 ± 0.015	-	-50 ± 15	0.950 ± 0.015
RT Wax Bolus	-	0.864	0.871 ± 0.003	-	-131 ± 3	0.869 ± 0.003
CT-ED Solid Water	-	1.046	1.016 ± 0.005	-	31 ± 5	1.031 ± 0.005
Water	-	1.000	1.000	-	-1.9 ± 29.6	1.000

Kim SY et al.(11) created a heterogeneous phantom replicating the commercial Rando phantom by combining plaster powder and polylactic acid (PLA) powder and determining the PLA powder percentage and infill value suitable for reproducing the soft tissue and mean bone HU values of the commercial Rando phantom. The bone tissue was altered using plaster and 0–35% PLA powder until an adequate HU value

was acquired, and the soft tissue was altered using PLA infill value until an appropriate HU value was obtained, in order to match the mean Hounsfield unit (HU) values of the Rando phantom. Figure 2.4a shows a picture that was taken after the top wall was taken off to show the cuboid specimens' infill. Figures 2.4b and c show CT images that were produced using various infill levels. The mean HU value in the CT image was checked using a region of interest (ROI). According to Figure 2.4b and Figure 2.4c, the ROI measured 4.5 cm horizontally and 0.6 cm vertically on the transversal plane and 4.5 cm square on the frontal plane, respectively. According to the infill value, Figure 2.5 displays the HU values. The standard deviation for an infill value of 5% is 88.8 HU. Also, a 100% infill value has a standard deviation of 11.5 HU. The inside of the cuboid specimen gets more uniform as the infill value decreases because it causes the standard deviation to decrease in value.

The 3D printer's mean HU value was adjusted by altering the ratio of the air volume to the printed thermoplastic volume, so the smaller the infill value, the less uniform it became. The Pearson correlation coefficient (r) was 0.999, indicating a linear relationship between the mean HU value and the infill value. The mean HU value, which ranged from 884.4 HU at an infill value of 5% to 169.0 HU at an infill value of 100%, represents the physical properties of plaster.

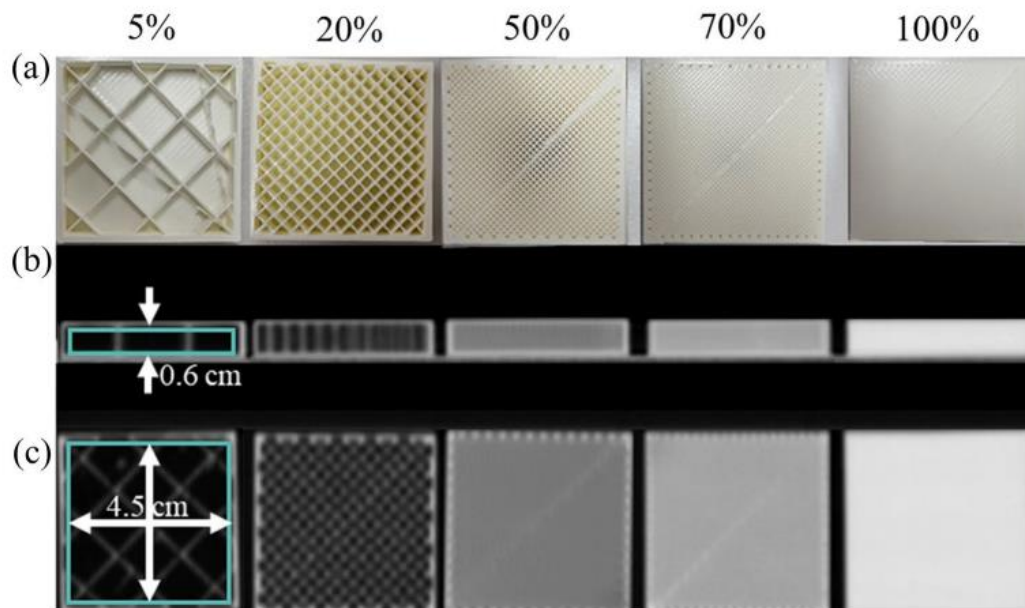


Figure 2. 4 (a) Photograph of cuboid specimens with infill of 5%, 20%, 50%, 70%, and 100%. (b) Images of the cubic phantom in the transverse and (c) frontal planes with infill from a CT scan.

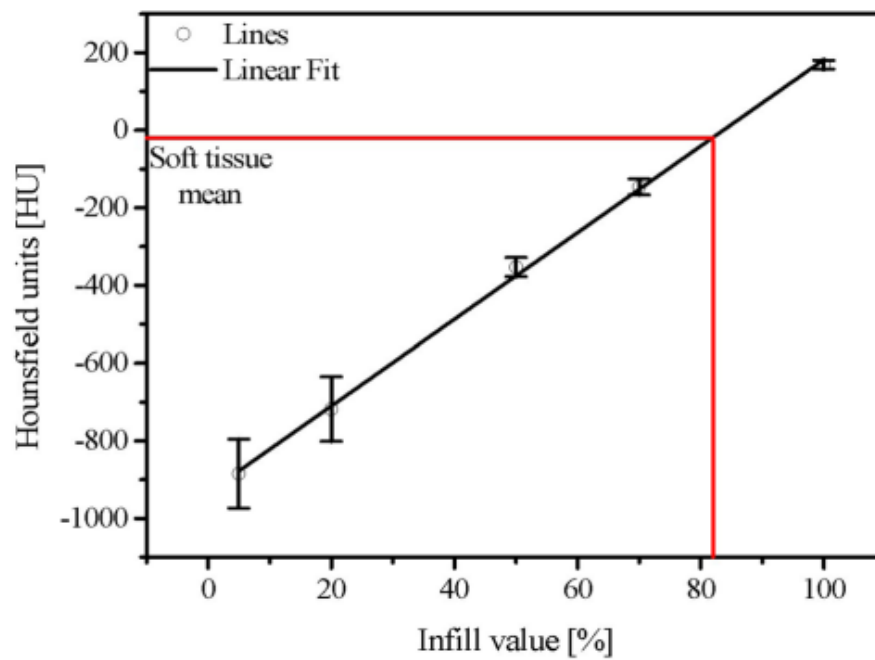


Figure 2. 5 Mean HU values depend on the 3D printer infill values.

CHAPTER III

RESEARCH METHODOLOGY

3.1 Research design

This research was observational design in the type of analytical study.

3.2 Research design model

This research was divided into two major steps: In-house phantom design and clinical application. Figures 3.1 and 3.2 display the diagram of each step in this research according to the above explanation.

3.2.1 In-house phantom design

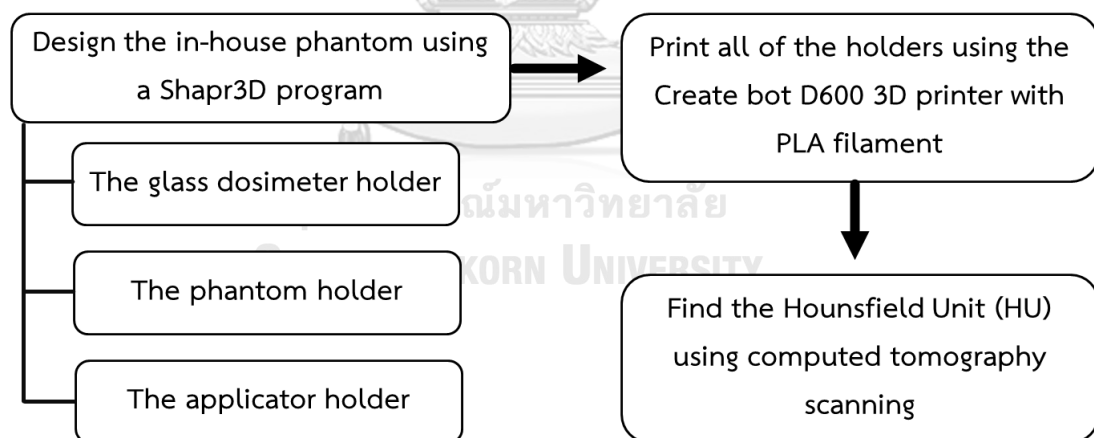


Figure 3.1 Research design model of In-house phantom design.

3.2.2 Clinical application

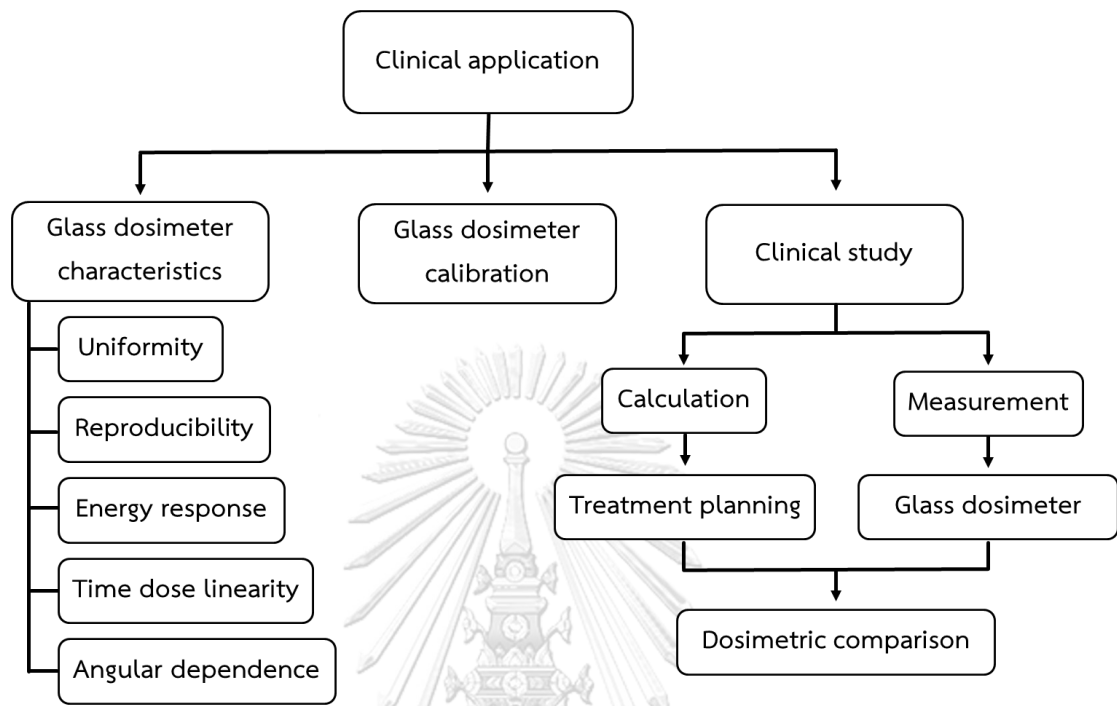


Figure 3.2 Research design model of clinical study.

3.3 Conceptual framework

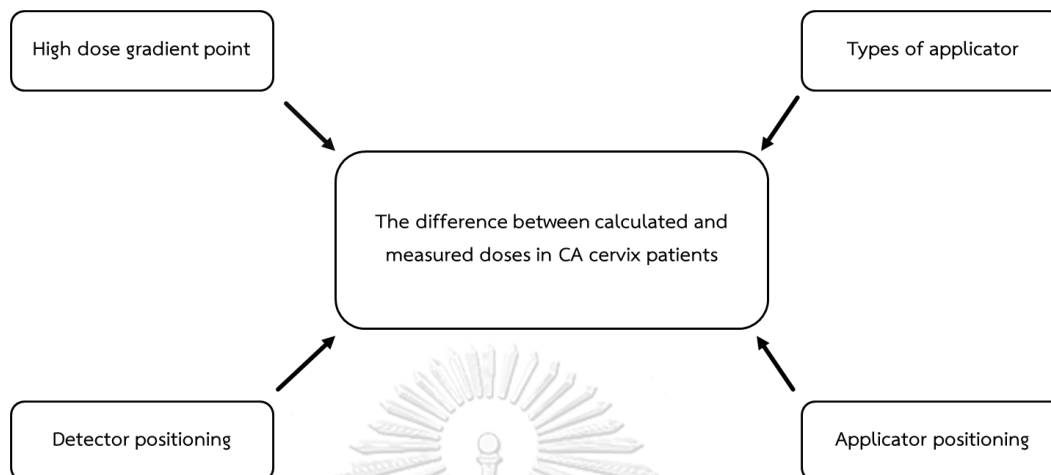


Figure 3.3 Conceptual framework.

3.4 Research questions

3.4.1 What are the dosimetric differences of 3D gynecological brachytherapy under clinical conditions between calculation and measurement using glass dosimeters in the in-house phantom?

CHULALONGKORN UNIVERSITY

3.5 Materials

The materials used in this study were supplied from the Division of Radiation Oncology, King Chulalongkorn Memorial Hospital.

3.5.1 The create bot D600 3D printer

The create bot D600 3D printer (Suwei Electronic Technology Co., Henan, China) is the fused deposition modelling (FDM) printing technology. It equipped with the 4th generation 1.75 mm filament diameter dual extruders and hotends(12). The

left extruder equipped with 260°C hotend, it is able to print with PLA, ABS, PC, Nylon, Carbon fiber, Flexible, etc. The right extruder 420 °C hotend is made of martensite steel, which is able to print high-performance materials. Moreover, the extruder feeding system support high-speed printing, and accuracy can reach high to 0.05 mm. The 3D printer is used to print out the In-house phantom, as shown in figure 3.4.



Figure 3.4 The create bot D600 3D printer.

3.5.2 PLA Filament

Polylactic acid (PLA) filament (Palawatr company, Sampran, Nakhon Pathom) is the thermoplastic monomer that is one of the most popular 3D printing materials due to its ease of use and low cost. The filament diameter is 1.75 mm with the density of 1.24 g/cm³, tensile strength of 50 MPa, flexural strength of 80 MPa and extremely low shrinkage with near-zero warping(13), as shown in figure 3.5.



Figure 3.5 PLA filament.

3.5.3 Shapr3D program

Shapr3D (Siemens Parasolid, Budapest, Hungary) is a cloud-based 3D CAD application, which enables the creation of geometric models on self-intersecting surfaces through complex calculations. It can do the creation of symmetrical lines, circles, and arcs and combines separate entities using subtract, union, and intersect Boolean formulas, and enables to export of 3D models in multiple file formats including STL, X_T, STEP, IGES, DXF, JPG, and PNG(14). The Shapr3D program is used to design the In-house phantom, as shown in figure 3.6.

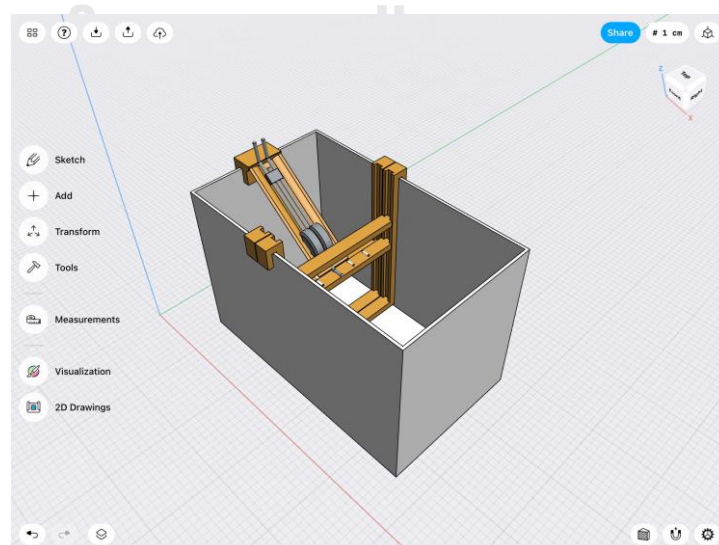


Figure 3.6 Shapr3D program

3.5.4 The GE CT simulator

A 512-slice GE Revolution CT scanner (GE Healthcare, Milwaukee, WI) is a CT simulator as shown in figure 3.7 installed on the B1 floor of Rattana Wittayaphat Building, King Chulalongkorn Memorial Hospital. The gantry of the Revolution CT machine has a diameter of about 80 cm, a full 50 cm scan field, scan of up to 200 cm with a table capacity of up to 675 lbs, enabling access to a wider range of patients. The tube voltage setting is 70, 80, 100, 120, and 140 kV with variable slice thickness from 0.625 mm to 1.25 mm(15).



Figure 3.7 The GE CT simulator.

3.5.5 Elekta Flexitron afterloader

Flexitron (Elekta AB, Stockholm, Sweden) is used to insert a radioactive source directly into a tumor, where it stays for a short time. This form of treatment delivers a precise, localized dose of radiation while minimizing exposure to healthy tissue, designed to simplify and enhance High Dose Rate (HDR) Brachytherapy treatments using Iridium-192(16), as shown in figure 3.8.



Figure 3.8 Elekta Flexitron afterloader.

3.5.6 The Fletcher applicator

A Fletcher CT/MR applicator (Nucletron, Elekta AB, Stockholm, Sweden), for intracavitary brachytherapy, the tandem lengths were adjustable by changing the position of the base according to the depth of the uterus. Ovoid diameters varied from 15 to 20 mm. The applicators will be placed with the tandem being placed through the cervix and into the uterus. The ovoid or ring is placed in the vagina and against the cervix, as shown in figure 3.9.



Figure 3.9 The Fletcher applicator.

3.5.7 Oncentra treatment planning system

Oncentra treatment planning system (Elekta AB, Stockholm, Sweden) is the component to generate a deliverable brachytherapy procedure, which is executed on the Flexitron remote afterloader treatment system(17). Any planning procedure has the competing objectives of optimal target coverage, dose homogeneity, and protection of organs at risk, as shown in figure 3.10.

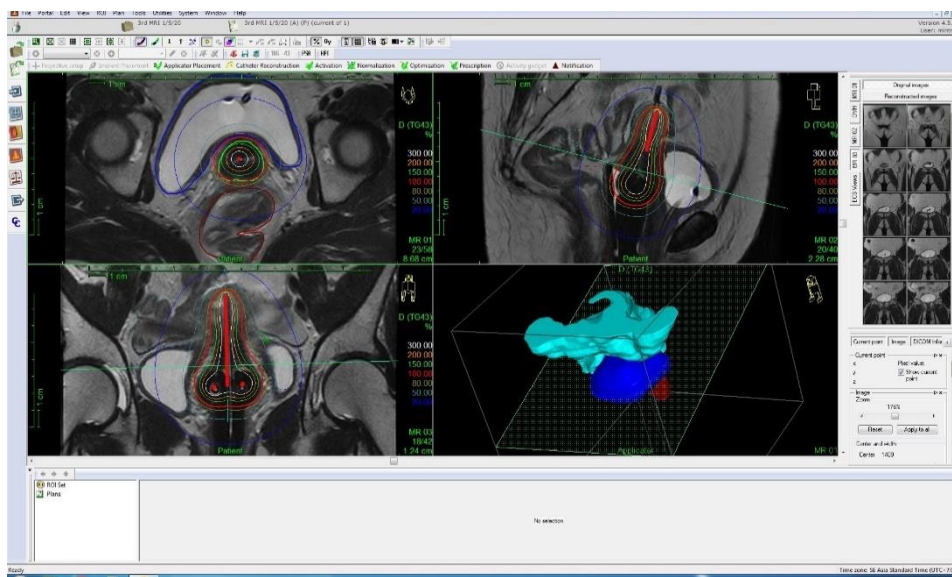


Figure 3.10 Oncentra treatment planning system.

CHULALONGKORN UNIVERSITY

3.5.8 Linear accelerator

The external beam radiation treatments machine is the Varian TrueBeam linear accelerator (Varian Medical System, Palo Alto, CA) or Linac, as shown in Figure 3.11. A linear accelerator is used to treat cancer patients. This Varian TrueBeam linear accelerator provides two photon energies of 6 MV and 10 MV in both flattened and unflattened photon beams(18). It can deliver high-energy electrons to the region of the patient's tumor. TrueBeam rotates around the patient to deliver a prescribed radiation dose from nearly any angle. In addition, the electron beams are also

provided in various energies of 6, 9, 12, 15, 18, and 22 MeV with an accessory called a multileaf collimator (MLC) that shapes the beam.



Figure 3.11 Varian TrueBeam linear accelerator.

3.5.9 PMMA phantom for brachytherapy

A PMMA cylindrical after-loading phantom, type 9193 (PTW, Saxony, Germany) or the Krieger phantom, is a cylindrical PMMA phantom in which the Ir-192 HDR source is positioned at the center and measured in the periphery by a calibrated thimble ionization chamber(19). It is used to check the Ir-192 HDR source with an independent instrument that measures a quantity closer to what is of interest in brachytherapy, this phantom has a diameter of 20 cm and a height of 12 cm. It consists of four peripheral holes at 8 cm radius from the center, as shown in figure 3.12.

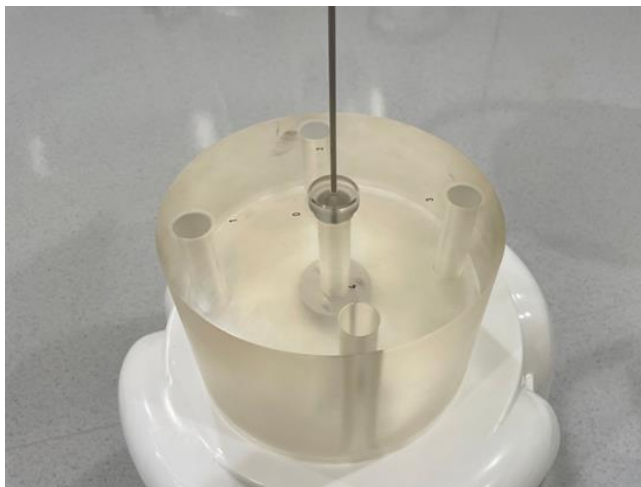


Figure 3.12 PMMA cylindrical after-loading phantom

3.5.10 Solid water phantom

The solid water phantom (Gammex, Middleton, WI) is a durable water equivalent phantom for photon and electron energy measurements. Water equivalence within 0.5% for therapeutic and diagnostic energy ranges ensures high precision with 30 cm x 30 cm in sizes and various thicknesses as displayed(20) in figure 3.13 are used in radiotherapy for routine dosimetric quality assurance tests, primarily due to their ease of use compared to scanning water tanks.



Figure 3.13 Solid water phantom

3.5.11 FC-65G and DOSE-I electrometer

The ionization chamber FC-65G (IBA Dosimetry GmbH, Schwarzenbruck, Germany) along with the DOSE-I electrometer (IBA Dosimetry GmbH, Schwarzenbruck, Germany), as displayed in figure 3.14 were utilized to measure the collected charge to calibrate the glass detector. FC65-G ionization chamber is intended for reference dosimetry and calibrations, the chamber is designed preferably for the energy ranges of photons and electrons at accelerators(21). The DOSE-I is a portable, single-channel, high-precision reference class electrometer, with easy-to-use functionality, the electrometer can be used with ionization chambers, semiconductor detectors, and diamond probes for measurements of absorbed dose.



Figure 3.14 FC-65G and DOSE-I electrometer

3.5.12 The radio-photoluminescence glass dosimeter (RPLGD)

The radio-photoluminescence glass dosimeter (RPLGD) (Asahi Techno Glass Co., Shizuoka, Japan), is a glass compound with a luminescent material. The size of a glass dosimeter is 1.5 mm and 12 mm in length, as shown in figure 3.15. RPLGDs have several advantages such as a wide dose measurement range from 10 μ Gy to 500 Gy,

a small fading effect of 0.4% after 100 days, and repeatable readouts. In particular, the RPLGD without a Tin filter called GD-302 M has been generally used in the quality assurance (QA) processes of radiotherapy units(22).

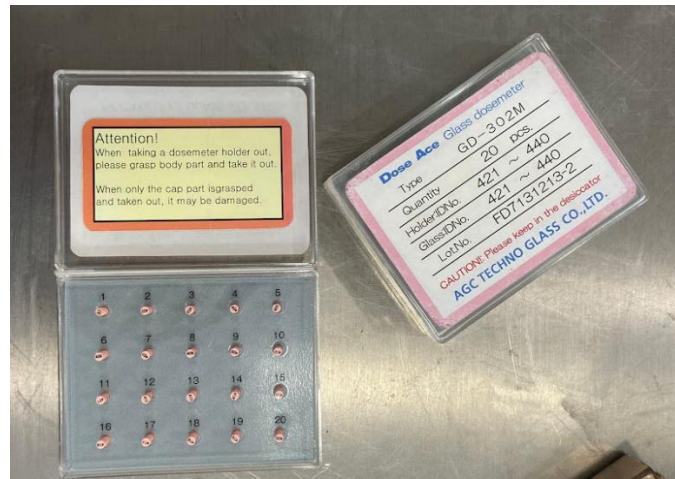


Figure 3.15 The radio-photoluminescence glass dosimeter (RPLGD).

3.5.13 The automatic reader FGD-1000

The reader (FGD-1000, Chiyoda Technol Co., Oarai, Japan) is the high sensitivity reader with the nitrogen gas laser as a source of ultraviolet light excitation which can perform a continuation pulse oscillation. It is possible to read out continuously 20 samples(23), it is possible to measure doses in the standard dose range (10 μ Gy-10 Gy) and high-dose range (1 Gy-500 Gy), as shown in figure 3.16.



Figure 3.16 The automatic reader FGD-1000.

3.5.14 Carbolite Gero

Carbolite Gero (Carbolite Gero Ltd, Neuhausen, Germany), as displayed in figure 3.17. Carbolite Gero's extensive chamber furnace range has a maximum operating temperature from 30°C to 3000°C and chamber capacities of up to 725 liters, excellent quality, and longevity(24), used to heat the glass detector after the dose reading.



Figure 3.17 Carbolite Gero.

3.6 Methods

The methods were divided into two sections. The first part was to design the in-house phantom. The second part was the section on comparing dosimetric differences in the clinical study.

3.6.1 In-house phantom design

The in-house phantom consists of a water tank made from acrylic, with dimensions: 22 cm x 38 cm x 25 cm, and accessories including the RPLGDs holder (Figure 3.18 (a)), the phantom holder (Figure 3.18 (b)), and the applicator holder (Figure 3.18 (c)). These holders were movable designed, can move along a length axis of 35 cm and glass holders can move along a height of 23 cm, and the axis of the holder was moved to represent the rectum points that differ according to the patient's anatomy. In addition, the holder of the applicator was designed for various types of applicators in intracavitary brachytherapy

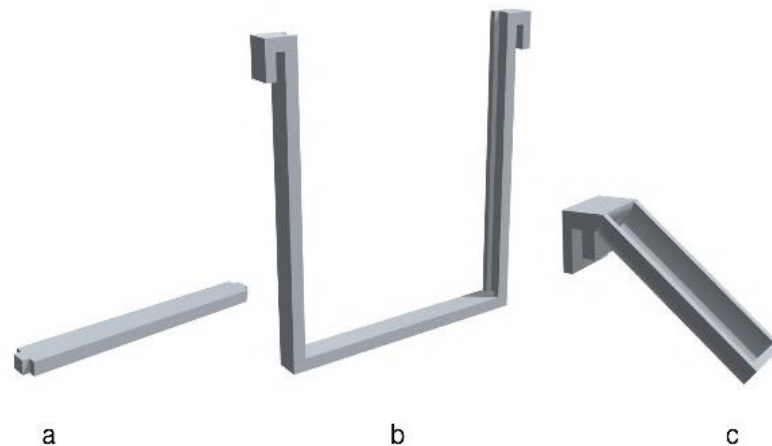


Figure 3.18 An illustration of the in-house phantom designed in Shapr3D, (a) the glass dosimeter holder, (b) the phantom holder, and (c) the applicator holder.

3.6.1.1 3D customized in-house phantom

The procedures of the 3D customized in-house phantom were as followings:

1. All the holders were designed together using a Shapr3D program (Siemens Parasolid, Budapest, Hungary), as shown in figure 3.19. The size and shape of the glass dosimeter holder was designed to 19 cm in length, 2 cm in width, 1 cm in height, and 1 cm in thickness. The phantom holder was designed as a suitable size with a water tank, 21 cm in length, 2 cm in width, 24 cm in height, and 1 cm in thickness. The applicator holder was designed as a 5 cm in diameter, 18 cm in length cylinder.

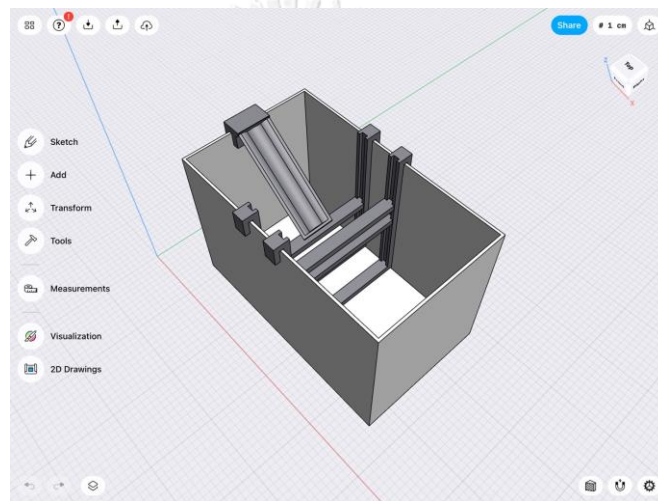


Figure 3.19 The design of all the holders.

2. These accessories were converted from STL files to G-code files in CreatWare V6.4.3. (SuWei Inc., Chongqing, China), and printed using a rectilinear pattern and an infill density of 30% by the create bot D600 3D printer using PLA Filament with a diameter of 1.75 mm, a very rigid material, and more common than other materials used in 3D printing, as shown in figure 3.20. The printing time of glass dosimeter holder, phantom holder, and the applicator holder were 2, 8, and 10 hours, respectively.

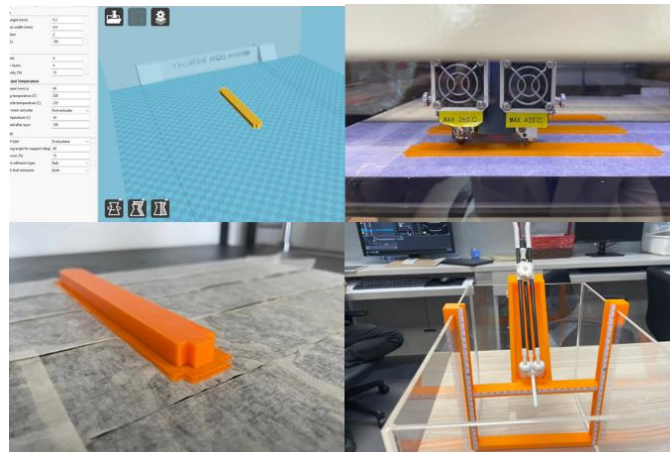


Figure 3.20 All the holders of the in-house phantom in the 3D printer process.

3. The in-house phantom was characterized using computed tomography scanning (Figure 3.21) to find the Hounsfield Unit (HU). CT images of the in-house phantom were obtained using a 512-slice GE Revolution CT scanner. The CT scanning conditions were as follows: 2.5 mm slice thickness, 120 kV, and 210 mAs.

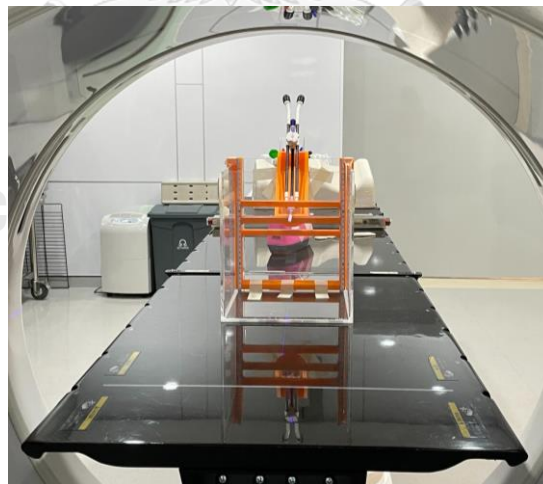


Figure 3.21 The in-house phantom setup in the CT scanner.

3.6.2 Clinical application

The clinical application consists of three parts: glass dosimeter characteristics, glass dosimeter calibration, and dosimetric evaluation in the clinical study.

3.6.2.1 Glass dosimeter characteristics

The experiments of RPLGD characteristics in uniformity and reproducibility were undertaken on 6-MV photon beams from Varian TrueBEAM. The energy dependence was undertaken on 6-MV and 10-MV photon beams from linear accelerator and 0.38 MeV gamma rays from Ir-192 source. The time dose linearity and angular dependence were undertaken on Flexitron HDR afterloader. The setting up condition of the glass dosimeter characteristic experiments; the field size was set to 10 cm x 10 cm, the source-to-surface distance (SSD) was adjusted to 100 cm, and the depth of measurement was set to 1.5 cm, as shown in figure 3.22.



Figure 3.22 The RPLGD setup position for each experiment.

3.6.2.1.1 Uniformity and reproducibility of RPLGD

To examine the uniformity study, 30 RPLGDs were exposed to 100 cGy. The automatic reader FGD-1000 was employed to read the RPLGD signal. The signals were read ten times for each dosimeter. For the reproducibility of the glass dosimeter, 10 RPLGDs were exposed to 100 cGy, the measurement was repeated three times.

3.6.2.1.2 Energy response

To investigate the energy response, the RPLGDs was irradiated with a similar dose level of 200 cGy from 6, and 10 MV photon beams from Linac and 0.38 MeV gamma rays from Ir-192 source.

3.6.2.1.3 Time dose linearity

For the time dose linearity, the RPLGDs was inserted in the cavity plug at the peripheral side of the cylindrical PMMA phantom for brachytherapy at position 9 O'clock (Figure 3.23). The Ir-192 source was inserted into the center of the cylindrical PMMA phantom for brachytherapy. The doses at 0.5, 1, 2, 5, 8, and 10 Gy were delivered to the RPLGDs.

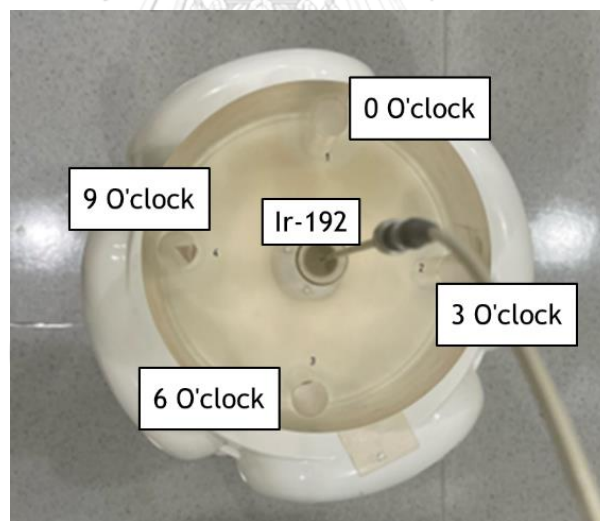


Figure 3.23 The setup position of the glass dosimeter, and Ir-192 inside the cylindrical PMMA phantom for brachytherapy.

3.6.2.1.4 Angular dependence

For the angular dependence study, the glass dosimeter was inserted in the cavity plug at the peripheral side of the cylindrical PMMA phantom for brachytherapy

in positions 0, 3, 6, and 9 O'clock, respectively (Figure 3.23). The Ir-192 source was inserted into the center of the cylindrical PMMA phantom for brachytherapy. The dose of 100 cGy was delivered to the RPLGDs.

3.6.2.2 Glass dosimeter calibration

To calibrate the RPLGD, the Flexitron Ir-192 source was inserted into the center of the cylindrical PMMA phantom, the RPLGD was inserted into the cavity plug at the peripheral side of the cylindrical PMMA phantom, and the ionization chamber FC-65G was inserted at the opposing side of the glass dosimeter, as shown in figure 3.24. The ionization chamber was connected to the DOSE-I electrometer to measure the radiation dose of 2 Gy at the same distance of 8 cm with RPLGD in the opposite side at the same time to validate the accuracy of the measured dose from the RPLGD.

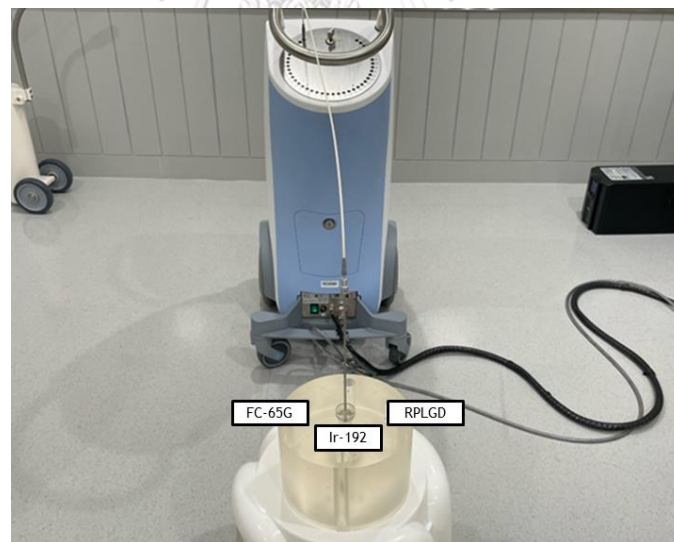


Figure 3.24 The setup position of RPLGD calibration in the cylindrical PMMA phantom.

3.6.2.3 Clinical study

The procedures of the clinical study were as followings:

1. The RPLGDs were attached to the holder of the in-house phantom at various points, as shown in figure 3.25, and were immersed into a water phantom. The reference point of the RPLGD was divided into point A, point B, bladder point, and rectum point. Point A is defined as 2 cm above the cervical os point (flange) and 2 cm lateral to midline (tandem), this point is used to measure the dose of radiation delivered to the tumor and surrounding tissues. Point B is defined as 3 cm laterally to point A, this point is used to evaluate the tumor's extent and estimate the dose received by the surrounding tissues. The bladder reference point is 2 cm above the ovoids and multiple rectal reference points as shown in figure 3.25, the RPLGD located at the center of the holder is labeled as R1, with the four other RPLGDs labeled as R2 to R5, and the distance between each point was taken as 1 cm, These points are used to monitor the doses of radiation that these organs receive during brachytherapy treatment.
2. The in-house phantom with a Fletcher CT/MR applicator was scanned by a 512-slice GE Revolution CT scanner as shown in figure 3.21, and transferred to the Oncentra Brachytherapy treatment planning system. Applicator configurations that were used for patient treatment based on the adopted departmental at the King Chulalongkorn Memorial Hospital protocol were simulated with the in-house phantom.

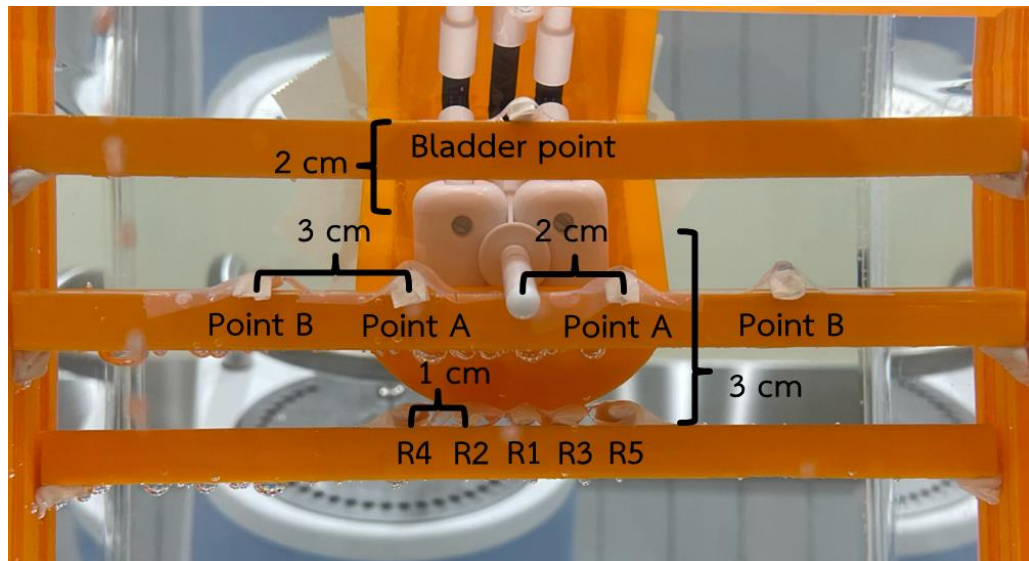


Figure 3.25 The setup position of the RPLGDs at various points in the in-house phantom, which included point A, point B, bladder, and rectum points.

3. The 6 gynecological retrospective plans were exported to the in-house phantom, in which the radiation oncologist contoured the high-risk clinical target volume (HR-CTV), bladder, and rectum on transverse slices according to GEC-ESTRO(25) and prescribed the dose of 8 Gy at HR-CTV, therefore the point A for this study dose depends on the volume of HR-CTV.

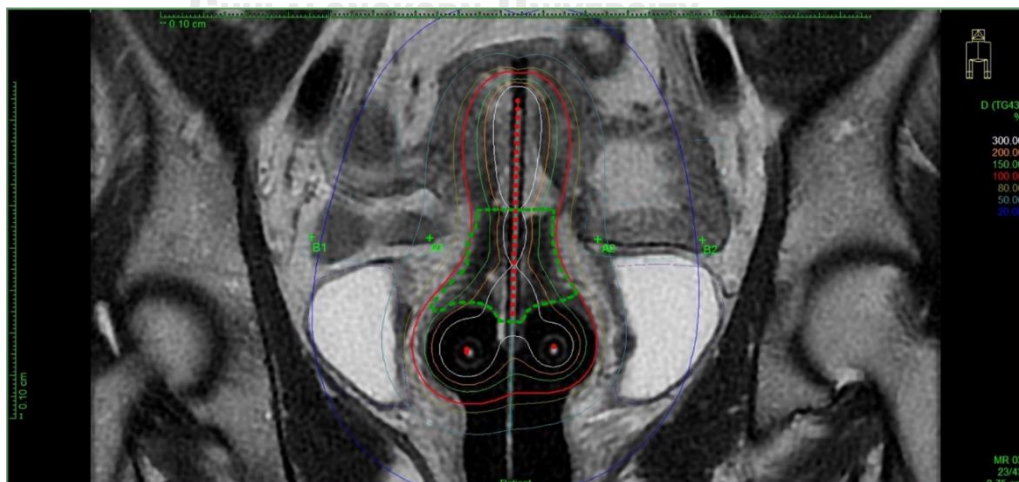


Figure 3. 26 The isodose distribution for the patient plan entered into the in-house phantom.

4. Six patients, who have previously been treated with 3 fractions of 8 Gy HDR intracavitary brachytherapy, and treated with the Fletcher applicator or Utrecht applicator without interstitial at the King Chulalongkorn Memorial Hospital, for cervical cancer were randomly selected to evaluate the dosimetric differences of gynecological brachytherapy under clinical conditions between calculation by the treatment planning system and measurement by glass dosimeters, and the measurement was performed and repeated three times.

3.7 Statistical analysis

1. Mean, and standard deviation were used to present the results.
2. The percentage dose differences defined as

$$\Delta D(\%) = \left(\frac{D_{\text{measured}} - D_{\text{planned}}}{D_{\text{planned}}} \right) \times 100$$

3.8 Sample size determination

The sample size was determined such that the average difference between doses measured with the Glass dosimeter and planned doses was 0.91 Gy and 0.41 SD [6] The sample size can be calculated by using the following equation:

$$n = \frac{\left(z_{1-\frac{\alpha}{2}} + z_{1-\beta} \right)^2 \sigma^2}{\Delta^2}$$

Where:

For $\alpha = 0.05$, $z_{1-\frac{\alpha}{2}} = 1.959964$

For $\beta = 0.10$, $z_{1-\beta} = 1.281552$

σ^2 is variance of difference ≈ 0.41 [6]

d is difference of mean = 0.91 Gy [6]

Solve equation

$$n = \frac{(1.959964 + 1.281552)^2 0.41^2}{0.91^2}$$

$$n = 3$$

3.9 Outcome measurement

The differences of calculated doses from the treatment planning system by using computed tomography images and *in vivo* measured dose by the RPLGD of an in-house phantom during high-dose-rate intracavitary brachytherapy treatment.

3.10 Benefits of research

To assess clinical IVD and investigates error detection for real-time treatment monitoring such as deviations between the delivered and planned dose.

3.11 Ethical consideration

This research involves the dosimetric differences between calculation and measurement using glass dosimeters in the in-house phantom. The patient plan data were collected and recalculated in phantom on the treatment planning system. The research proposal was submitted and approved by Institutional Review Board (IRB) of Faculty of Medicine, Chulalongkorn University, and Bangkok, Thailand (IRB NO.0457/65). The certificate is shown in APPENDIX.

CHAPTER IV

RESULTS

The results were separated into two sections. The first part was to design the in-house phantom. The second part was the section on comparing dosimetric differences in the clinical study.

4.1 In-house phantom design

The HU of the in-house phantom was measured with a sufficient region of interest (ROI) at 4 points including, the applicator (tandem and ovoid), the holder (PLA material), and the water tank. The comparison of the in-house phantom with the properties of 3D-printed materials is summarized in Table 4.1, with listing the types of material and Hounsfield units (HU) values. The HU values of the in-house phantom were 144 HU for tandem and 267 HU for ovoid. The PLA 3D-printed phantom was -631 HU.

Table 4.1 Measured Hounsfield unit (HU) for various parts of applicators and PLA material.

Materials	HU
Tandem	144 ± 5.6
Ovoid	267 ± 6.3
Air	-996 ± 2.8
Water	0
PLA	-631 ± 19.0

4.2 Clinical application

The clinical application consists of three parts, glass dosimeter characteristics, glass dosimeter calibration, and comparison of dosimetric differences in the clinical study.

4.2.1 Glass dosimeter characteristics

The results of glass dosimeter characteristics consist of five parts, uniformity, reproducibility, energy response, time dose linearity, and angular dependence.

4.2.1.1 Uniformity

The uniformity reading from 30 RPLGDs is presented in Figure 4.1. The relative response of all RPLGD was $\pm 1.32\%$, The lowest relative response was 0.97 and the highest was 1.03 for the 100 cGy dose.

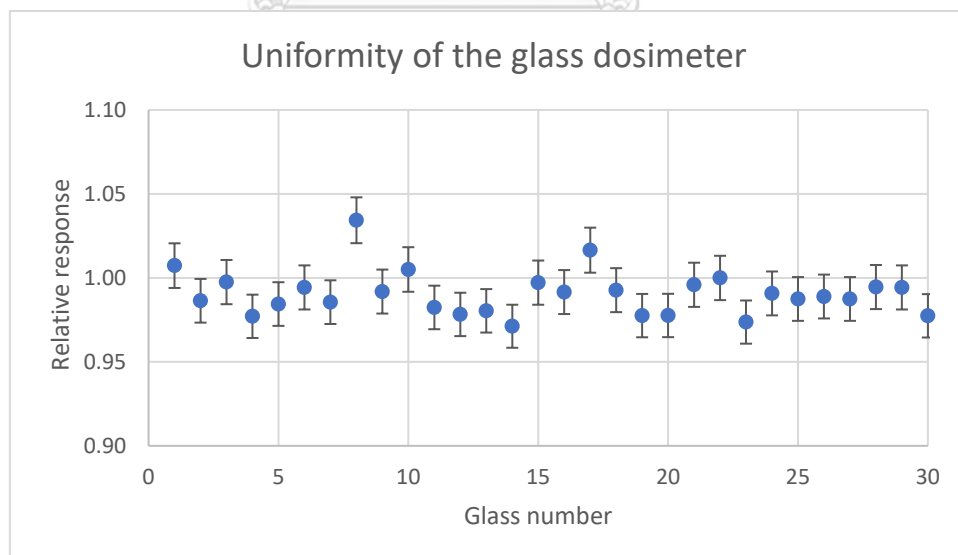


Figure 4.1 The uniformity of 30 RPLGDs at the dose of 100 cGy. The error bars show the standard deviation from 10 times readout.

4.2.1.2 Reproducibility

The reproducibility of the RPLGDs was studied with three times repeated measurements from 10 RPLGDs. The relative response was normalized to the average signal of 10 RPLGDs. The results are shown in Figure 4.2. Overall, the average of the relative response was $1.00 \pm 1.69\%$ which indicated that the glass dosimeter was very stable.

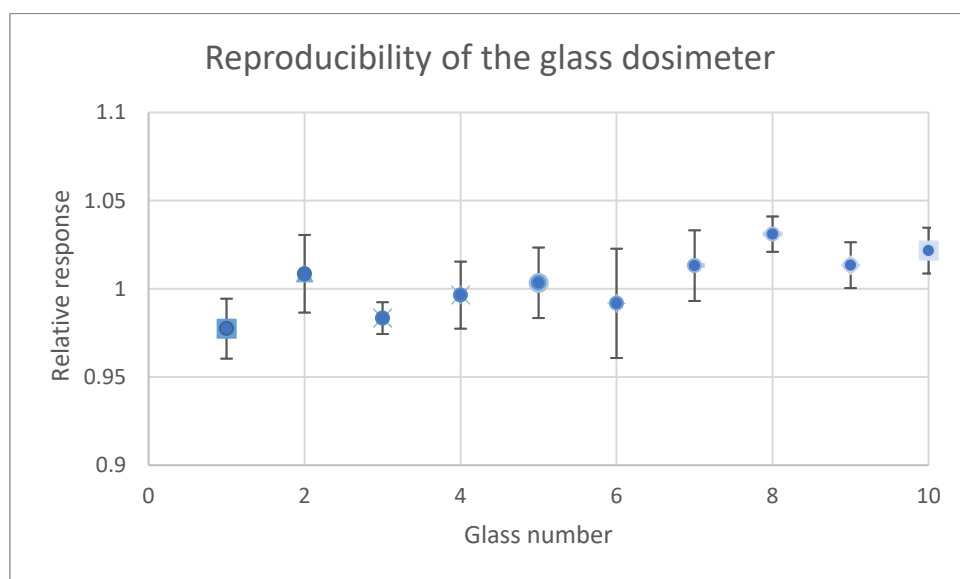


Figure 4.2 The reproducibility of the RPLGD. The error bars display the standard deviation from measurements that were taken three times.

4.2.1.3 Energy response

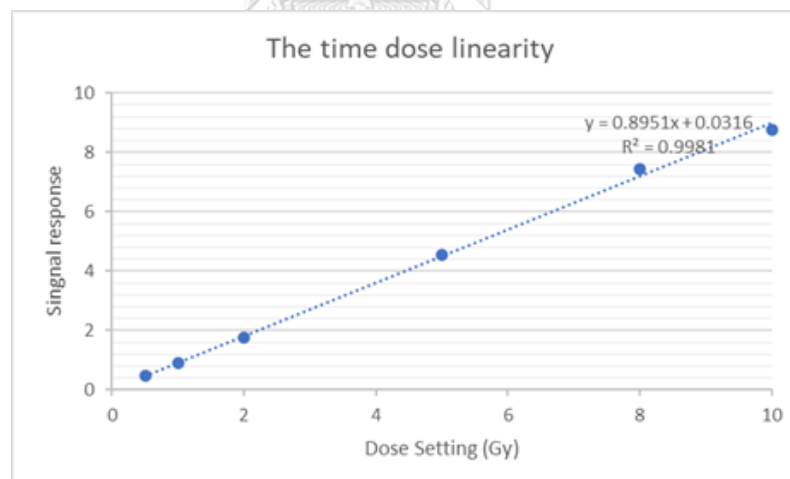
Table 4.2 summarizes the difference of energy response of RPLGD from various high-energy photon beams and γ -rays from the Ir-192 source. relative to 6 MV photon beams. The maximum relative response was 0.966 ± 0.02 for 0.38 MeV, indicating that the RPLGD is energy independence to high-energy photon beams from Linac and 0.38 MeV γ -rays from the Ir-192 source.

Table 4.2 Difference of energy response to the RPLGD.

Energy	Relative response to 6 MV
6 MV (Linac)	1.000 ± 0.07
10 MV (Linac)	0.989 ± 0.04
0.38 MeV (Ir-192)	0.966 ± 0.02

4.2.1.4 Time dose linearity

For the time dose linearity, as shown in Figure 4.3, the RPLGD response yielded a linear proportion over the dose range from 0.5 to 10 Gy with the R^2 of 0.998.

**Figure 4.3** The time dose linearity response of RPLGD.

4.2.1.5 Angular dependence

Figure 4.4 presents the angular dependence of the RPLGD at various angles. The relative response was normalized to the RPLGD readout of the axis at 0° gantry

angle. Each point displayed the outcome from the average of three repeated measurements and five times readout in each glass dosimeter. In positions 0, 3, 6, and 9 O'clock the RPLGD response was similar.

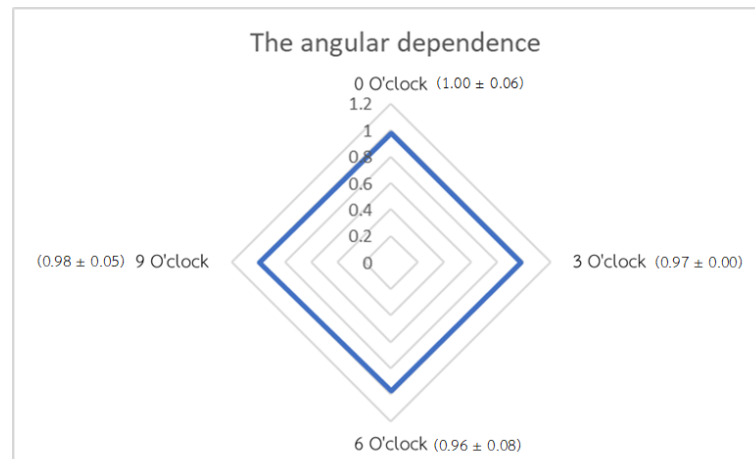


Figure 4.4 The angular dependence of the RPLGD at different positions in the cylindrical PMMA phantom.

4.2.2 Glass dosimeter calibration

For the ionization chamber FC-65G, the air Kerma rate from measurement was 35.79 mGy/h which was 0.3% difference from the certification (35.89 mGy/h). The RPLGDs comparison between the calculated and measured dose had the acceptable dose difference at 2.4% which was lesser than 5% of the recommended limitation in the report from ESTRO Booklet No. 8(26).

4.2.3 Clinical study

Table 4.3 illustrates the results of the measurement using the glass dosimeter at point A in the phantom medium and the dose differences between calculation and measurement. The mean dose difference for planned numbers 1-6 at point A

were $2.16 \pm 1.51\%$, $2.4 \pm 1.53\%$, $3.27 \pm 0.86\%$, $1.35 \pm 0.32\%$, $1.68 \pm 0.93\%$, and $1.08 \pm 0.91\%$ respectively. The mean dose difference compared to the calculated dose for planned 1-6 at point A was $1.99 \pm 1.11\%$, which has an acceptable difference between the measured and TPS calculated dose was within $\pm 5\%$ of the recommended from TRS-430(27).

Table 4.3 Comparison between dose calculation and measurement at point A.

Number	Dose	Point A (L)	Point A (R)
1	Calculated dose (Gy)	2.56	2.56
	Measured dose (Gy)	2.64 ± 0.14	2.53 ± 0.32
	ΔD (%)	3.23	-1.09
2	Calculated dose (Gy)	2.94	3.04
	Measured dose (Gy)	2.91 ± 0.10	3.15 ± 0.08
	ΔD (%)	-1.32	3.48
3	Calculated dose (Gy)	3.38	3.42
	Measured dose (Gy)	3.51 ± 0.05	3.52 ± 0.21
	ΔD (%)	3.88	2.66
4	Calculated dose (Gy)	4.17	4.17
	Measured dose (Gy)	4.22 ± 0.03	4.24 ± 0.09
	ΔD (%)	1.12	1.57
5	Calculated dose (Gy)	3.52	3.48
	Measured dose (Gy)	3.60 ± 0.41	3.52 ± 0.16
	ΔD (%)	2.33	1.02
6	Calculated dose (Gy)	6.92	6.90
	Measured dose (Gy)	6.95 ± 0.26	7.02 ± 0.54
	ΔD (%)	0.43	1.72

Table 4.4 illustrates the results of the measurement using the glass dosimeter at point B in the phantom medium and the dose differences between calculation and measurement. Point B receives a low dose since the dose gradient was steeply close to the source's location it showed the value was higher percentage than the calculated dose in advance in planned numbers 1,2,3, and 5. However, the absolute dose difference for planned numbers 1-6 at point B were 0.04 ± 0.00 Gy, 0.13 ± 0.02 Gy, 0.15 ± 0.01 Gy, 0.06 ± 0.04 Gy, 0.13 ± 0.01 Gy, and 0.07 ± 0.01 Gy respectively.

Table 4.4 Comparison between dose calculation and measurement at point B.

Number	Dose	Point B (L)	Point B (R)
1	Calculated dose (Gy)	0.48	0.48
	Measured dose (Gy)	0.52 ± 0.01	0.52 ± 0.01
	ΔD (%)	7.56	8.55
2	Calculated dose (Gy)	0.80	0.80
	Measured dose (Gy)	0.91 ± 0.01	0.94 ± 0.03
	ΔD (%)	13.44	16.92
3	Calculated dose (Gy)	0.80	0.80
	Measured dose (Gy)	0.96 ± 0.02	0.94 ± 0.05
	ΔD (%)	19.76	16.98
4	Calculated dose (Gy)	1.04	1.04
	Measured dose (Gy)	1.07 ± 0.05	1.05 ± 0.01
	ΔD (%)	2.56	0.93
5	Calculated dose (Gy)	0.80	0.80
	Measured dose (Gy)	0.93 ± 0.02	0.92 ± 0.01
	ΔD (%)	16.25	15.40
6	Calculated dose (Gy)	1.60	1.60
	Measured dose (Gy)	1.66 ± 0.03	1.68 ± 0.01
	ΔD (%)	3.98	4.71

Table 4.5 illustrates the results of the measurement using the glass dosimeter at the bladder point in the phantom medium and the dose differences between calculation and measurement. The mean dose difference for planned numbers 1-6 at the bladder point were 4.00%, 2.94%, 9.17%, 2.71%, 3.59%, and 3.71% respectively, which has an acceptable difference between the measured and TPS calculated dose was within $\pm 5\%$ of the recommended from TRS-430(27), excluding plan number 3 that higher percent than the calculated dose due to position error from unintentionally moved by setting up the glass dosimeter in individual measurements. The mean dose difference compared to the calculated dose for planned 1-6 at the bladder point was $4.42 \pm 2.56\%$.

Table 4.5 Comparison between dose calculation and measurement at bladder point.

Number	Dose	Bladder
1	Calculated dose (Gy)	1.76
	Measured dose (Gy)	1.83 ± 0.02
	ΔD (%)	4.00
2	Calculated dose (Gy)	2.08
	Measured dose (Gy)	2.14 ± 0.01
	ΔD (%)	2.94
3	Calculated dose (Gy)	2.40
	Measured dose (Gy)	2.62 ± 0.07
	ΔD (%)	9.17
4	Calculated dose (Gy)	2.88
	Measured dose (Gy)	2.96 ± 0.04
	ΔD (%)	2.71
5	Calculated dose (Gy)	2.56
	Measured dose (Gy)	2.65 ± 0.28
	ΔD (%)	3.59

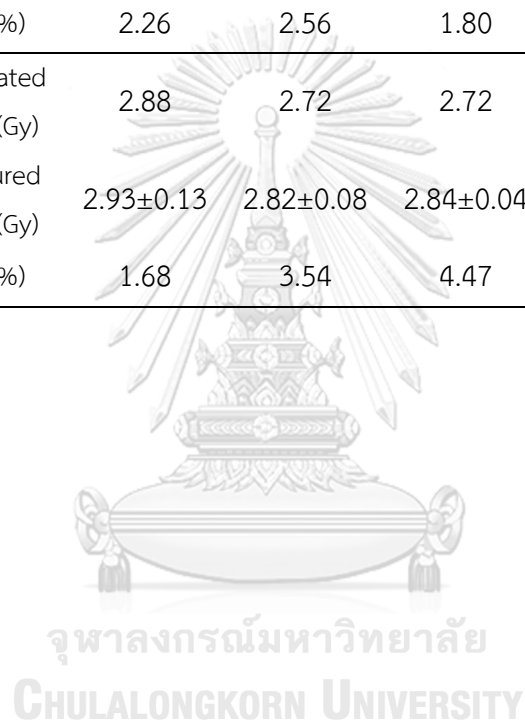
	Calculated dose (Gy)	4.80
6	Measured dose (Gy)	4.98 ± 0.09
	ΔD (%)	3.71

Finally, table 4.6 illustrates the results of the measurement using the glass dosimeter at the rectum point in the phantom medium and the dose differences between calculation and measurement. The mean dose difference for planned numbers 1-6 at the rectum point were 3.88±2.07%, 4.42±1.98%, 2.96±6.51%, 3.52±0.29%, 3.22±1.42%, and 3.18±1.07% respectively. The mean dose difference compared to the calculated dose for planned 1-6 at the rectum point was 3.53±1.44%, which has an acceptable difference between the measured and TPS calculated dose was within ±5% of the recommended from TRS-430(27).

Table 4.6 Comparison between dose calculation and measurement at rectum point.

Number	Dose	R1	R2	R3	R4	R5
1	Calculated dose (Gy)	1.12	1.12	1.12	0.96	0.96
	Measured dose (Gy)	1.13±0.05	1.16±0.02	1.16±0.04	1.01±0.01	1.02±0.01
	ΔD (%)	0.92	3.40	3.76	4.72	6.63
2	Calculated dose (Gy)	1.60	1.44	1.45	1.21	1.28
	Measured dose (Gy)	1.65±0.04	1.35±0.03	1.54±0.03	1.23±0.02	1.33±0.02
	ΔD (%)	3.31	-6.36	6.55	1.96	3.94
3	Calculated dose (Gy)	1.60	1.44	1.45	1.28	1.28
	Measured dose (Gy)	1.68±0.02	1.51±0.04	1.47±0.04	1.33±0.02	1.32±0.02
	ΔD (%)	4.79	4.36	1.18	3.46	2.85

4	Calculated dose (Gy)	1.92	1.94	1.76	1.60	1.60
	Measured dose (Gy)	2.00±0.03	2.01±0.03	1.82±0.03	1.66±0.04	1.65±0.02
	ΔD (%)	3.95	3.46	3.50	3.59	3.12
5	Calculated dose (Gy)	1.76	1.60	1.63	1.44	1.44
	Measured dose (Gy)	1.80±0.06	1.64±0.05	1.66±0.02	1.51±0.02	1.50±0.04
	ΔD (%)	2.26	2.56	1.80	4.99	4.49
6	Calculated dose (Gy)	2.88	2.72	2.72	2.24	2.25
	Measured dose (Gy)	2.93±0.13	2.82±0.08	2.84±0.04	2.32±0.04	2.31±0.05
	ΔD (%)	1.68	3.54	4.47	3.63	2.59



CHAPTER V

DISCUSSION AND CONCLUSION

5.1 Discussion

5.1.1 In-house phantom design

The in-house phantom consists of the RPLDG holder, the phantom holder, and the applicator holder (Figure 3.18). All of these were constructed with a 3D printer using PLA material, the most commercially available printer. In the 3D-printed phantom, the Hounsfield Unit or HU was measured using computed tomography scanning, the HU value of PLA material was -631 ± 19.0 HU, which was consistent with the value from Van der Walt M et al.(10) of -693 ± 17 HU. Due to the 30% of material infill density in the printed process, there were slight differences between the HU from Van der Walt M et al.(10), and Sung Kim SY et al.(11) have expanded the investigation of the HU values according to the infill density. As the infill value decreases, the value of the standard deviation decreases, meaning that the inside of the cuboid specimen becomes more uniform. Although the HU was different, it had no effect on the dose measurements since this experiment was performed in water, and the HU for water was 0 HU, which is closer to the soft tissue (+20 to +40 HU) and the phantom post-print was not taken long to print and it was high stiffness and strength to hold and affix a glass dosimeter with the water tank.

5.1.2 Glass dosimeter characteristics

We investigated whether the RPLGD might be utilized as an in-vivo dosimeter for brachytherapy., the measurements were carried out using an in-house phantom intended for verifications in cervical cancer treatment using brachytherapy. The reproducibility of the glass dosimeter in our study was $\pm 1.6\%$ which good agreement with the reported by Oonsiri P et al.(28). where they discovered the value of $\pm 1.5\%$. Our research found the uniformity was $\pm 1.3\%$ at the dose of 100 cGy, which is

consistent with a result from Arakia F et al.(29) where they discovered the value of $\pm 1.1\%$. The time dose linearity measured in this study, showed an R^2 of 0.998 that was in good agreement as compared to Phurailatpam R et al.(30) where they found R^2 of doses from 0.5 to 10 Gy was 0.997. The RPLGDs offer excellent characteristics for radiation dosimetry.

5.1.3 Clinical study

In this study, only the Fletcher applicator was used, hence the treatment plan chosen was in the 8 Gy range, which when adapted plan to the phantom, the calculated dose will be in the medium dose rate range. The dose differences between calculation and measurement are shown in Table 4.3. The dose differences between the calculated and measured dose at point A showed values of 0.43-3.88%, which has an acceptable difference between the measured and TPS calculated dose was within $\pm 5\%$ of the recommended from TRS-430(27). The mean dose difference compared to the calculated dose for planned 1-6 at point A was $1.99 \pm 1.11\%$, which was in good agreement with the results published by Moon SY et al.(6) where they discovered the mean dose difference of $3.85 \pm 2.6\%$.

Point B receives a low dose since the dose gradient was steeply close to the source's location, as shown in figure 3.26 illustrating the isodose distribution for the patient plan entered into the in-house phantom. The HR-CTV in the green dotted line prescribed an 8 Gy dose. As can be observed, reference point A is far from the HR-CTV, hence the calculated dose is not equal to the prescribed dose, and reference point B is far from the source, resulting in a low dose. Table 4.4 showed the value was higher percent than the calculated dose in advance. However, the absolute dose difference for planned numbers 1-6 at point B was about 0.1 Gy. In table 4.5, the mean dose differences between calculation and measurement at the bladder point for plans 1-6 were $4.42 \pm 2.56\%$, the measured dose at rectum points in Table 4.6, the

mean dose difference from all cases was $3.53 \pm 1.44\%$ which agreed well with the reported from Nose T et al.(9) where they discovered the mean dose difference of $3.85 \pm 2.18\%$ for bladder point and $3.82 \pm 2.67\%$ of the rectum point.

5.2 Conclusion

In conclusion, using 3D printing technology and PLA material has allowed for the creation of highly effective and affordable internal phantoms for use in brachytherapy. The glass dosimeter holder, phantom holder, and applicator holder have all been designed adjustable, taking into account the patient's anatomy and allowing for accurate measurements at various points. While there may be slight variations in dose calculation, the difference between the calculated and measured dose for most points was within 5% of the recommended. Due to the high dose gradient in brachytherapy resulting from the radioactive source being placed close to the target tissue, causing the radiation dose to drop off rapidly in surrounding tissues, hence point B received a low dose, the value was a higher percentage than the calculated dose in advance, however, the absolute dose difference was approximately 0.1 Gy. Overall, we consider that in-vivo dosimetry in the in-house phantom using the RPLGD for brachytherapy can minimize overdoses and provide an accurate record of the actual delivered dose for the patient using an accessory for the applicator in clinical practice.

REFERENCES

1. Bour BK IS, Tagoe SNA, Amuasi JH, Sasu E, Hasford F. Dose assessment in high dose rate brachytherapy with cobalt-60 source for cervical cancer treatment: a phantom study. *Polish J Med Phys Eng.* 2020;26(4):243-50.
2. Tanderup K, Beddar S, Andersen CE, Kertzscher G, Cygler JE. In vivo dosimetry in brachytherapy. *Med Phys.* 2013;40(7):070902.
3. Uptodate. Brachytherapy for low-risk or favorable intermediate-risk, clinically localized prostate cancer [Internet]. [cited 2022 Aug 11]. Available from: <https://www.medilib.ir/uptodate/show/6923>.
4. Nikoofar A, Hoseinpour Z, Rabi Mahdavi S, Hasanzadeh H, Rezaei Tavirani M. High-Dose-Rate (192)Ir Brachytherapy Dose Verification: A Phantom Study. *Iran J Cancer Prev.* 2015;8(3):e2330.
5. IAEA. Optimization in brachytherapy [Internet]. [cited 2023 Apr 18]. Available from: <https://www.iaea.org/resources/rpop/health-professionals/radiotherapy/Brachytherapy/optimization>.
6. Moon SY, Son J, Yoon M, Jeang E, Lim YK, Chung WK, et al. Applicability of Glass Dosimeters for In-vivo Dosimetry in Brachytherapy. *Korean Phys Soc.* 2018;72(11):1320-5.
7. Hashimoto S, Nakajima Y, Kadoya N, Abe K, Karasawa K. Energy dependence of a radiophotoluminescent glass dosimeter for HDR 192 Ir brachytherapy source. *Med Phys.* 2018;46(2):964-72.
8. All3DP. The 7 Main Types of 3D Printing Technology [Internet]. [cited 2023 Apr 18]. Available from: <https://all3dp.com/1/types-of-3d-printers-3d-printing-technology/>.
9. Nose T, Koizumi M, Yoshida K, Nishiyama K, Sasaki J, Ohnishi T, et al. In vivo dosimetry of high-dose-rate interstitial brachytherapy in the pelvic region: use of a radiophotoluminescence glass dosimeter for measurement of 1004 points in 66 patients with pelvic malignancy. *Int J Radiat Oncol Biol Phys.* 2008;70(2):626-33.
10. Van der Walt M, Crabtree T, Albantow C. PLA as a suitable 3D printing thermoplastic for use in external beam radiotherapy. *Australas Phys Eng Sci Med.* 2019;42(4):1165-76.

11. Kim SY, Park JW, Park J, Yea JW, Oh SA. Fabrication of 3D printed head phantom using plaster mixed with polylactic acid powder for patient-specific QA in intensity-modulated radiotherapy. *Sci Rep.* 2022;12(1):17500.
12. CreatBot. D600 Pro Affordable and Reliable Large 3D printer [Internet]. [cited 2023 Apr 18]. Available from: <https://www.creatbot.com/en/creatbot-d600.html>.
13. NRAS. 3D PRINTER Filament [Internet]. [cited 2023 Apr 18]. Available from: <https://www.nras.co.th/3d-printer-filament.php>.
14. GetApp. Shapr3D Pricing, Features, Reviews and Alternatives [Internet]. [cited 2023 Apr 18]. Available from: <https://www.getapp.com/construction-software/a/shapr3d/>.
15. Healthcare G. Revolution CT [Internet]. [cited 2023 Apr 18]. Available from: <https://www.gehealthcare.co.uk/products/computed-tomography/revolution-family/revolution-ct>.
16. Center BC. Elekta Flexitron [Internet]. [cited 2023 Apr 18]. Available from: <https://www.basscancercenter.com/cancer-treatment-technology/elekta-flexitron>.
17. Elekta. Oncentra Brachy [Internet]. [cited 2023 Apr 18]. Available from: <https://www.elekta.com/products/brachytherapy/oncentra-brachy/>.
18. Varian. TrueBeam [Internet]. [cited 2023 Apr 18]. Available from: <https://www.varian.com/products/radiotherapy/treatment-delivery/truebeam>.
19. Johan SK, Lobo D, Athiyamaan MS, Srinivas C, Banerjee S, Abhishek K, et al. In-vivo Comparison of Planned and Measured Rectal Doses during Cobalt-60 HDR CT-based Intracavitary Brachytherapy Applications of Cervical Cancer Using the PTW 9112 Semiconductor Probe. *Asian Pac J Cancer Prev.* 2023;24(3):897-907.
20. Nuclear S. Solid Water [Internet]. [cited 2023 Apr 18]. Available from: <https://www.sunnuclear.com/products/solid-water-he>.
21. Dosimetry I. FC65-G / FC65-P Ionization Chambers [Internet]. [cited 2023 Apr 18]. Available from: <https://www.iba-dosimetry.com/product/fc65-g-fc65-p-ionization-chambers>.
22. Kim JS, Park BR, Yoo J, Ha W-H, Jang S, Jang WI, et al. Measurement uncertainty analysis of radiophotoluminescent glass dosimeter reader system based on GD-352M for estimation of protection quantity. *Nuc Eng and Tec.* 2022;54(2):479-85.

23. CROSBY. Glass rod dosimeter in patient dosimetry Chambers [Internet]. [cited 2023 Apr 18]. Available from: <https://www.bib.irb.hr/734796>.
24. Carbolite. Carbolite Gero [Internet]. [cited 2023 Apr 18]. Available from: <https://www.carbolite-gero.com/>.
25. Potter R LE, Wambersie A. Reporting in Brachytherapy: Dose and Volume Specification. GEC-ESTRO Handbook of Brachytherapy.
26. Bidmead M BE, Burger J, Ferreira I, Grusell E, Kirisits C, et al. . A practical guide to quality control of brachytherapy equipment. BOOKLET NO. 8.
27. AGENCY IAE. Commissioning and Quality Assurance of Computerized Planning Systems for Radiation Treatment of Cancer, Technical Reports Series No. 430, IAEA, Vienna, (2004).
28. Oonsiri P, Kingkaew S, Vannavijit C, Suriyapee S. Investigation of the dosimetric characteristics of radiophotoluminescent glass dosimeter for high-energy photon beams. J Radiat Res Appl Sci. 2019;12(1):65-71.
29. Arakia F, Moribe N, Shimonobou T, Yamashita Y. Dosimetric properties of radiophotoluminescent glass rod detector in high-energy photon beams from a linear accelerator and cyber-knife. Med Phys. 2004;31(7):1980-6.
30. Phurailatpam R, Upreti R, Nojin Paul S, Jamema SV, Deshpande DD. Characterization of commercial MOSFET detectors and their feasibility for in-vivo HDR brachytherapy. Phys Med. 2016;32(1):208-12.

APPENDIX

The approval of institutional review board

Certificate approval from institutional review board (IRB) of Faculty of Medicine,
Chulalongkorn University, Bangkok, Thailand.



COA No. 0007/2023
IRB No. 0457/65

INSTITUTIONAL REVIEW BOARD
Faculty of Medicine, Chulalongkorn University
1873 Rama 4 Road, Pathumwan, Bangkok 10330, Thailand, Tel 662-256-4493

Certificate of Full Board Approval
(COA No. 0007/2023)

The Institutional Review Board of the Faculty of Medicine, Chulalongkorn University, Bangkok, Thailand, has approved the following study in compliance with the International guidelines for human research protection as Declaration of Helsinki, The Belmont Report, CIOMS Guideline and International Conference on Harmonization in Good Clinical Practice (ICH-GCP)

Study Title : In vivo dosimetry of In-house phantom using the RPLGD in 3D Gynecological brachytherapy

Study Code : -

Principal Investigator : Miss Itsaraporn Konlak

Affiliation of PI : Department of Radiology,
Faculty of Medicine, Chulalongkorn University.

Review Method : Full board

Continuing Report : At least once annually or submit the final report if finished.



Document Reviewed :

1. Research Proposal Version 4.0 Date 29 December 2022
2. Protocol Synopsis Version 4.0 Date 29 December 2022
3. Case Record Form Version 3 Date 26 November 2022
4. Curriculum Vitae and GCP Training
- Miss Itsaraporn Konlak

Figure A The approval of institutional review board



- Asst.Prof. Dr. Taweap Sanghangthum
- Dr. Mintra Keawsamur
- Mrs. Chulee Vannavijit
- Mr. Sakda Kingkaew
- Petch Alisanant, M.D.
- Miss Nichakan Chatchumnan

Signature  (Emeritus Professor Tada Sueblinvong MD) Chairperson The Institutional Review Board	Signature  (Associate Professor Wannarasmi Ketchart MD, PhD) Member and Assistant Secretary, Acting Secretary The Institutional Review Board
------------------------------------------------------------------------------------------------------------------------------------------------------------------------------------------	-----------------------------------------------------------------------------------------------------------------------------------------------------------------------------------------------------------------------------------------

Date of Approval : January 12, 2023
 Approval Expire Date : January 11, 2024

Figure B The approval of institutional review board



VITA

NAME Itsaraporn Kontak

DATE OF BIRTH 6 May 1999

PLACE OF BIRTH Ratchaburi, Thailand

INSTITUTIONS ATTENDED Bachelor of Science, Department of Applied Radiation and Isotopes, Faculty of Science, Kasetsart University, Bangkok, Thailand

